

Detection of Coronary Artery Blockage at an Early Stage using Effective Deep Learning Technique

By:

Tahmid Ashrafee Promit

18301068

Md. Akibur Rahman Khan

18301050

Nahian Arnob

21301749

Rabbi Nur Rashid

21301715

Afif Reza

21301599

A thesis submitted to the Department of Computer Science and Engineering in
partial fulfillment of the requirements for the degree of B.Sc. in Computer Science
and Engineering

Department of Computer Science and Engineering
Brac University
September 20, 2022

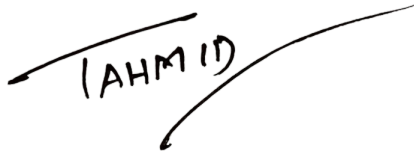
© 2022. Brac University
All rights reserved.

Declaration

It is hereby declared that

1. The thesis submitted is our own original work while completing degree at Brac University.
2. The thesis does not contain material previously published or written by a third party, except where this is appropriately cited through full and accurate referencing.
3. The thesis does not contain material which has been accepted, or submitted, for any other degree or diploma at a university or other institution.
4. We have acknowledged all main sources of help.

Student's Full Name & Signature:



Tahmid Ashrafee Promit
18301068



Md Akibur Rahman Khan
18301050



Nahian Arnob
21301749



Rabbi Nur Rashid
21301715



Afif Reza
21301599

Approval

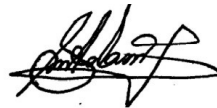
The thesis/project titled “Detection of Coronary Artery Blockage at an Early Stage using Effective Deep Learning Technique” submitted by

1. Tahmid Ashrafee Promit (18301068)
2. Md Akibur Rahman Khan (18301050)
3. Nahian Arnob (21301749)
4. Rabbi Nur Rashid (21301715)
5. Afif Reza (21301599)

Of Summer, 2022 has been accepted as satisfactory in partial fulfillment of the requirement for the degree of B.Sc. in Computer Science on September 22, 2022.

Examining Committee:

Supervisor:
(Member)



Md. Ashraful Alam, PhD
Assistant Professor
Department of Computer Science and Engineering
Brac University

Program Coordinator:
(Member)

Md. Golam Rabiul Alam, PhD
Professor
Department of Computer Science and Engineering
Brac University

Head of Department:
(Chair)

Sadia Hamid Kazi
Chairperson and Associate Professor
Department of Computer Science and Engineering
Brac University

Abstract

A coronary artery blockage is a form of coronary artery disease also known as CAD. It is the most common and frequent disease affecting the human body over the age of 65. CAD is a type of cardiovascular disease that happens because of a disorder in the coronary arteries of the human heart. Stenosis is the abnormal narrowing of the coronary artery due to the buildup of cholesterol which results in poor blood circulation causing a blockage. The development of computer science technologies has made drastic changes in medical science practices that include cardiology. Such advancements have made the invention of medical tests like Angiogram, Electrocardiogram, Magnetic Resonance Imaging, Echocardiogram, etc. These are imaging techniques to visualize arterial and venous vessels throughout the body for the diagnosis of various diseases. In common medical practice, the analysis and diagnosis of CAD mainly rely on the visual inspection and calculation of measurements by experienced cardiologists and doctors. Our proposed method aims toward a fully automated system for detecting a coronary artery blockage at an early stage using image processing and deep learning techniques so that the system can help doctors as well as patients to improve the medical treatment of the heart at an early stage. The goal of this research is to implement a system that can detect stenosis areas of the coronary artery due to the buildup of cholesterol plaque and other blocking agents. To examine stenosis in the coronary artery, Angiogram images are essential. Evaluating 2,151 Angiogram Image Dataset we train and test our models to reach a conclusion. The research uses CNN architecture models that use a dataset of 2D Angiogram images of the segmented coronary arteries which are analyzed using VGG16, VGG19, ResNet50, InceptionV3, and DenseNet121 models. To enhance our study, we classified our dataset into two classes i.e Binary Classification and Multiclass Classification. Next, using Ensemble model architecture, we evaluate the results and accuracy of the models used in the procedure of identifying coronary artery blockage. We used evaluation metrics Accuracy, Precision, Recall, and F1 Score to evaluate our results. Finally, we achieved accuracy, precision, recall, and F1 Score of more than 0.99 for the Binary Classification and more than 0.98 for the multiclass classification respectively of our dataset. In this way, the use of deep learning techniques can improve and develop medical science at a prodigious level resulting in error-free medical treatment of the heart at an early stage.

Index terms: Stenosis, Coronary Artery, Deep Learning, VGG, ResNet, Inception, DenseNet, Ensemble, Segmentation, Classification, Angiogram.

Dedication

This paper is dedicated to all the members, the faculties, the doctors, and every single person who has worked and supported to bring this research paper together in one piece. Their dedication and contribution have made this possible so far.

Acknowledgement

First and foremost, all praise to the **Almighty Allah** for whom our thesis has been completed without any major interruption. Secondly, we express immense gratitude to our thesis supervisor **Dr. Md. Ashrafal Alam**, Assistant Professor, Department of Computer Science and Engineering, Brac University and our mentor, **Shakib Mahmud Dipto**, Research Assistant, Department of Computer Science and Engineering, Brac University for their kind support and guidance which helped us all the way from the beginning till the end. We would also like to thank **Prof. Dr. Md. Mostafizur Rahman Ratan**, Professor of Cardiology, BSMMU and **Dr. Nurjahan Ananna**, Senior Medical Officer, ICU, CPH for their valuable time, helping us process our dataset and giving us knowledge about Cardiology. Thirdly, we would like to thank our parents. Without their continuous encouragement, we would not be able to progress as far as we have.

Lastly, our remarkable teamwork has led us to finish this research and thesis paper with an inspiration to move forward in our life.

Nomenclature

CAD - Coronary Artery Disease
CTA - Computed Tomography Angiogram
VGG - Visual Geometry Group
XAI - Explainable Artificial Intelligence
WHO - World Health Organization
ECG - Electrocardiogram
CNN - Convolutional Neural Network
RNN - Recurrent Neural Network
ResNet - Residual Neural Network
ReLU - Rectified Linear Unit
K-NN - K-Nearest Neighbors
FPGA - Field Programmable Gate Array
MATLAB - MATrix LABoratory
SVM - Support Vector Machine
MDCT - Multi-detector Computed Tomography
CBRBS - Cumulative Belief Rule-Based System
MIP - Maximal Implantation Potential
SSIM - Structural Similarity Index Measure
IOU - Intersection Over Union
CALD - Computer-Aided Logic Design
CReLU - Concatenated Rectified Linear Unit
SYNTAX - Set of rules defining the various combinations of symbols
MSCT - Multislice Computed Tomography
CT - Computed Tomography
AI - Artificial Intelligence
ILSVRC - Large Scale Visual Recognition Challenge
TP - True Positive
TN - True Negative
FP - False Positive
FN - False Negative
PCA - Principal Component Analysis
OpenCV - Open Source Computer Vision
LVQ - Learning Vector Quantisation
ML - Machine Learning
IEEE - Institute of Electrical and Electronics Engineers
SGD - Stochastic Gradient Descent
DNN - Deep Neural Network
DDSM - Digital Database for Screening Mammography
CV - Cross Validation
DCNN - Deep convolutional neural network
CIFAR - Canadian Institute for Advanced Research
FCN - Fully-Connected Network
MRI - Magnetic Resonance Imaging
SCNN - Segmentation and Classification Convolutional Neural Network
XRA - Exclusive OR Accumulator

Table of Contents

Declaration	i
Approval	ii
Abstract	iii
Dedication	iv
Acknowledgement	v
Nomenclature	vi
Table of Contents	vii
List of Figures	2
1 Introduction	4
1.1 Coronary Artery Blockage and its aftermath	4
1.2 Problem Statement	5
1.3 Aims and Objective	6
1.4 Research Orientation	6
2 Literature Review	7
3 Methodology	12
3.1 Architectures of Proposed Systems	12
3.2 Used Models and Architectures	15
3.2.1 ResNet50:	15
3.2.2 VGG16:	16
3.2.3 VGG19:	17
3.2.4 Inception V3:	17
3.2.5 DenseNet121:	18
3.2.6 Ensemble Model:	19
3.3 Convolutional Layer	19
3.3.1 Activation Function	19
3.4 Confusion Matrix	20
4 Implementation	22
4.1 Dataset	22
4.1.1 Source	22

4.1.2	Data Classification	22
4.2	Data Preprocessing	23
4.2.1	Data Labels	23
4.2.2	Image Resizing	24
4.2.3	Data Splitting	24
4.2.4	Normalization	24
5	Result and Analysis	25
5.1	Result and Analysis	25
5.2	Binary Classification	25
5.2.1	ResNet50	25
5.2.2	VGG16	26
5.2.3	VGG19	27
5.2.4	Inception V3	28
5.2.5	DenseNet121	29
5.2.6	Ensemble Model	30
5.3	Multiclass Classification	31
5.3.1	ResNet50	31
5.3.2	VGG16	32
5.3.3	VGG19	33
5.3.4	Inception V3	34
5.3.5	DenseNet121	35
5.3.6	Ensemble Model	36
5.4	Confusion Matrix	37
5.4.1	Binary Classification	37
5.4.2	Multiclass Classification	41
5.5	Result Analysis	45
5.6	Result Comparison	47
6	Conclusion and Future Prospect	49
	Bibliography	50

List of Figures

3.1	Proposed Architecture System Diagram	13
3.2	Binary Classification	14
3.3	Multiclass Classification	14
3.4	Residual Learning block	15
3.5	Internal Architecture of ResNet50	16
3.6	Internal Architecture of VGG16	16
3.7	Internal Architecture of VGG19	17
3.8	Internal Architecture of Inception V3	18
3.9	Internal Architecture of DenseNet121	18
3.10	Confusion Matrix	21
4.1	Healthy Heart Angiogram Image	23
4.2	Blocked Heart Angiogram Image	23
4.3	Blocked Heart Angiogram Image	23
5.1	Training curve(s) of ResNet50 architecture	25
5.2	Validation curve(s) of ResNet50 architecture	26
5.3	Training curve(s) of VGG16 architecture	26
5.4	Validation curve(s) of VGG16 architecture	27
5.5	Training curve(s) of VGG119 architecture	27
5.6	Validation curve(s) of VGG19 architecture	28
5.7	Training curve(s) of Inception V3 architecture	28
5.8	Validation curve(s) of Inception V3 architecture	29
5.9	Training curve(s) of DenseNet121 architecture	29
5.10	Validation curve(s) of DenseNet121 architecture	30
5.11	Training curve(s) of Ensemble Model architecture	30
5.12	Validation curve(s) of Ensemble Model architecture	31
5.13	Training curve(s) of ResNet50 architecture	31
5.14	Validation curve(s) of ResNet50 architecture	32
5.15	Training curve(s) of VGG16 architecture	32
5.16	Validation curve(s) of VGG16 architecture	33
5.17	Training curve(s) of VGG19 architecture	33
5.18	Validation curve(s) of VGG19 architecture	34
5.19	Training curve(s) of Inception v3 architecture	34
5.20	Validation curve(s) of Inception v3 architecture	35
5.21	Training curve(s) of DenseNet121 architecture	35
5.22	Validation curve(s) of DenseNet121 architecture	36
5.23	Training curve(s) of Ensemble model architecture	36
5.24	Validation curve(s) of Ensemble model architecture	37

5.25	Confusion Matrix of ResNet50	37
5.26	Confusion Matrix of VGG16	38
5.27	Confusion Matrix of VGG19	39
5.28	Confusion Matrix of Inception V3	39
5.29	Confusion Matrix of DenseNet121	40
5.30	Confusion Matrix of Ensemble Model Architecture	41
5.31	Confusion Matrix of ResNet50	41
5.32	Confusion Matrix of VGG16	42
5.33	Confusion Matrix of VGG19	43
5.34	Confusion Matrix of Inception V3	43
5.35	Confusion Matrix of DenseNet121	44
5.36	Confusion Matrix of Ensemble Model Architecture	45
5.37	Accuracy of Binary classification of different architectures	45
5.38	Comparison of Binary classification of different architectures	46
5.39	Accuracy of Multiclass classification of different architectures	46
5.40	Comparison of Multiclass classification of different architectures	47
5.41	Accuracy of Ensemble Model Architecture	47

Chapter 1

Introduction

1.1 Coronary Artery Blockage and its aftermath

The heart is the most prominent body organ of the human body. It maintains the blood flow process of the human body and is responsible for the circulation of blood in every organ of the body. The heart helps in blood circulation through the arteries and veins which circulate all over the body to keep every organ of the body functional. Blockage in such arteries is the primary reason that leads to CAD. CAD occurs when the oxygen-carrying blood arteries become clogged, preventing oxygenated blood and nutrients from reaching the heart. Heart muscles shrink as a result of this defect, and the major organ of the human body, the heart, loses its regular blood circulating ability [1]. The arteries are clogged due to the buildup of plaque, fatty deposits, and cholesterol which narrow the arteries decreasing regular blood flow to the heart muscles. Reduced blood flow may eventually result in a myocardial infarction also known as a heart attack [5,6]. Coronary Artery Disease is now regarded as the highest deadly disease for its higher fatality rate than other heart diseases. Approximately 1.8 crore people died in 2018, which results in 31% of all worldwide deaths (age under 70), and over 1.7 crore individuals died from diseases related to cardiology in 2017 as per statistics reported by WHO [2]. Furthermore, this number is steadily increasing. Diagnosis of coronary artery disease is done by performing several tests by doctors. These tests include ECG, Holter test, stress test, color doppler echo, and angiogram. Because ECG and treadmill tests are noninvasive in nature, as a result, due to many biases it cannot provide a reliable result for CAD [3]. Moreover, stress tests can be unpleasant for patients since one requires walking on a treadmill, which hampers the usual heart function. On the contrary, [4] coronary angiography is considered the most standard for finding CAD.

1.2 Problem Statement

Coronary Artery disease is identified as the most deadly disease that has caused the highest fatality to date than any other disease. It is ensured by statistics provided by WHO that, the death due to Cardiac diseases is gradually increasing since the year 2000. Thus, the cardiology sector in medical science needs drastic development to save mankind from such diseases.

More reasons are illustrated below;

- The conventional diagnosis of CAD is a lengthy and time-consuming process that endangers a patient at risk of death.
- Clinical diagnosis of coronary artery blockage is expensive and costly.
- The conventional approach has possibilities of human error.
- Patients have to undergo several tests and diagnoses for determining coronary artery diseases.
- Doctors require much time to detect the block accurately during the procedure of angiogram.
- Patients with stenosis less than 10-15% are mostly disregarded and ignored.

On the other hand, for financial benefit, numerous hospitals fabricate false reports that lead patients to unnecessary cardiac procedures. In an article by Peter E. Et al. [19] it was known that a semi-pro baseball player at the age of 30 had to undergo a pacemaker implant from a minor heart complexion which later was found could be treated with blood pressure medication. Later, the doctor carrying out the pacemaker implant was imprisoned in charge of billing dozens of unnecessary heart procedures. Similarly, innumerable times each year patients undergo surgeries that are not necessary at all. To conclude, medical science requires more development to eradicate such problems.

1.3 Aims and Objective

In our research, we proposed an efficient way to detect coronary artery blockage in the early stages using deep learning neural network methods. Here, we aim to prepare a deep learning model that can predict the accuracy of coronary artery blockage by analyzing the 2D Angiogram image dataset. Our prior objective is to determine the intensity of coronary artery blockage at an early stage to ensure obligatory precocious action that can save oneself from the danger of a heart attack. The remaining objective is as follows:

- Early detection of coronary artery blockage before it causes a heart attack.
- Understanding the use of deep learning techniques using CNN for medical science development.
- To develop a model for blockage detection based on Angiogram Image Segmentation, and analysis.
- Detect minor Stenosis and create future awareness for heart diseases.
- Bring Automation to the procedure of coronary blockage detection.

The uniqueness to our research is the approach of study and methodology. We have used a unique approach of analyzing the angiogram image dataset. As classification in machine learning, we have used multiclass classification along with binary classification. This approach helped us analyze the medical results in depth identifying each location of the block accurately. We analyzed every important artery of the heart in detail. We studied the different parts of the heart as in Right Coronary Artery RCA, Left Circumflex Artery LCX, Left Anterior Descending Artery LAD in our multiclass classification research. Furthermore, The multiclass classification is reducing the overfitting test set reuse issue. This multiclass classification can significantly determine the exact location of coronary blockage of the heart. As the system is trained significantly to identify each and every artery for the block. These are the few unique aspects of our model. In addition, we used five different models to test and train our dataset. Collectively, the results were summarized more accurately using Ensemble model architecture for precise accuracy of our complete work. To conclude, these are the few unique aspects of our research paper.

1.4 Research Orientation

In chapter 2, we reviewed past research about our field of study by a variety of researchers. After that, in chapter 3, we provided examples and descriptions for the algorithms, ResNet50, VGG16, VGG19, Inception V3, DenseNet121, and the Ensemble model that we have used during our research. Furthermore, we showed the use of our research and the distribution of our datasets in chapter 4. We have provided the findings of our investigation one more time in chapter 5. In chapter 6, we finally reached a conclusion and discussed related topics and future prospects as well.

Chapter 2

Literature Review

Salma S. Et al. [7] in their research paper stated about recognizing the narrowed coronary artery from the angiographic scanned images. They first employed filters to strengthen Coronary Artery Angiographic scans, then a region expanding algorithm to discover and segment these scans, and last a K-Nearest Neighbor classifier to categorize them as normal or abnormal cases. To discover Coronary Arteries, their proposed method comprises enhancing and reducing noise from Angiographic scan images. In actuality, their plan is divided into the following phases. Firstly, image preprocessing is done which comprises image enhancement and edge detection. Secondly, image segmentation. And then, picture categorization using the K-NN classifier. They used a total of 75 participants in their study, 60 of whom were abnormal and 15 of whom were normal. On this dataset, their technique properly detected 71 patients while wrongly diagnosing others. This result gave a 93.3 percent True Positive rate, suggesting that aberrant cases were successfully discovered 93.3 percent of the time. The false-negative rate is 6.6 percent. Their method correctly diagnosed other patients. Finally, they came to the conclusion that their prototype application was a trustworthy and accurate approach for cutting down on examination time. It improves, identifies, and speeds up coronary imaging diagnostics, and it achieves improved results by the methods they mentioned.

S. B. Mudigoudar Et al. [8] on their research used Angiogram or cardiac catheterization, a traditional approach to detect cardiac blockages. Cardiac blockages are identified using FPGA-implemented on Canny edge detector and Watershed image processing methods and visualizing the data on a screen and optimizing the proposed heart blockage detector in terms of speed, power, and area. Images of a cardiac angiography were taken with an X-ray and imaging system. The captured images are supplied into the operator block for input image coefficient preprocessing and memory storage. The initialization image coefficients are delivered to both the Edge detector and the Watershed algorithm block at the same time for the main processing of the preprocessed input picture. The basic method entails detecting and pinpointing the image's obstruction spot. The image complement block complements the edge detector and watershed block outputs to create a single image that depicts the obstruction detected output image. A set of comparators, registers, adders, and subtractors make up the watershed block. The thresholding values were compared to the pixel values in the comparators block. If the pixel is valued above the thresholding value, the output is zero; otherwise, the output is one. At the output image, the blended output leads to superior blockage detection. The

output of the picture complement is fed into the display unit's input. The specified images are displayed on the monitor. For cardiac blockage identification, canny edge detector and watershed image processing methods are used on both the MATLAB and FPGA platforms. The quality of the input image determines the accuracy. The design might potentially be used to detect cancer cells, according to the report, if appropriate image processing techniques are used.

According to the research of Roohallah A. Et al. [9] Angiography is the finest and most accurate way to diagnose coronary artery disease. Here, the data mining methods are used. They believe these algorithms have the capacity to precisely detect components that lead to cardiac disease. They also claimed that a patient having stenosis more than fifty percent has coronary artery disease. Meanwhile, they used applied Information Gain for the feature analysis. It was utilized to rank the characteristics according to their impact on artery stenosis. Subsequently, feature selection for the diagnosis of stenosis of every particular artery was done using SVM weights. Additionally, the RapidMiner tool version 5.2.003 was used to define the Information Gain of the dataset characteristics. The performance metric was calculated using a cross-validation technique. To Train the data set, cross-validation was used to pick features and tune parameters (C and). Next, the average combined information gain approach for feature selection was proposed in this study. There were 24 features chosen by each technique. The classification algorithm results revealed that these two approaches to feature selection were more accurate. However, SVM is an augmentation of the presented approach. First, the gap between the sample and the separating hyperplane is calculated. They decide not just on the symbol of the data, but also from the ap of the subspace, unlike SVM. They used four distinct distances based on four different SVM kernels (polynomial, sigmoid, linear, and RBF). Recall indicates the degree to which the results are complete. An algorithm with a high recall has retrieved the majority of the relevant results. Ultimately, the stenosis of the left anterior descending artery left circumflex artery, and right coronary artery arteries were investigated individually in this study. A new feature selection scheme was used to choose more preferential features to improve models even further. This method of feature selection was chosen because it performed better than others. This new method combined with the new algorithm produced the best accuracy for blockage detection of the left anterior descending artery, left circumflex artery, and right coronary artery: 86.14%, 83.17%, and 83.50%, respectively. These are the max accuracies found so far according to them. F'N, P'N, and R'N were presented as solutions for this. The F'N and R'N algorithms were more accurate than various SVM kernels. Finally, R'N was adopted for judgment in practical applications since it performed significantly better than F*N.

Carlo G. Et al. [10] describe a 64-slice MDCT method that is a precise intraoperative strategy. The contraction in the coronary arteries of patients with persistent ischemia disease is assessed using this technique. They have examined around 67 asymptomatic, high-risk hypertension individuals (Euro N5%). MDCT successfully points out (94%) individuals with severe CAD at a minimum of one vessel and (96%) others in the per-patient study. Multi-detector row tomography properly recognized (95%) coronary blockage of 50 percent and (98%) unblocked segments in the per-segment analysis, with a negative significant prognostic of traditional scans. It is

concluded that MDCT System is a good noninvasive approach for detecting severe coronary stenoses.

Sohrab Et al. [11] in their work described a method by which CBRBS can forecast various types of coronary artery disease. The suggested prototype CDSS can classify coronary artery disease CAD severity into four categories. At first, occlusion of almost any artery. Secondly, occlusion in particularly one artery. Thirdly, occlusion in two, and lastly, occlusion in three arteries. For these four types of CAD, the rate of success, rate of error, and rate of non-success are all calculated. The given system was successful in 93.97 percent of the time. The proposed approach can reduce the rate of error and failure from class two to class four. New categorization can be attached in the future to improve the classifier's effectiveness.

A research paper written by U. Rajendra Acharya Et al. [12] stated, a computerized process for detecting coronary artery disease has been proposed using various ECG segments with CNN based on an electrocardiogram, that is used to monitor cardiac healthiness. ECG signals are nonlinear and no stationary and transitory disease indications might appear at any point on the time scale, making this approach to treating an irregular hit difficult, time intensive, and prone to human error. ECG data can be collected in various ways. ECG signals vary by class in real life, depending on characteristics. To do it in the correct way some limits are to be followed to do deep learning on ECG signals. Finally, the authors came to the conclusion that because CAD escorts heart attacks, an automated diagnosis technique is both reliable and effective for detecting CAD early. Finally, they implemented a model with 94.95% accuracy. They believed that this new system will aid clinicians in an effective diagnosis of CAD. In addition, it is an easy to use and inexpensive procedure and can be utilized for cardiac screening in underdeveloped countries.

Abdallah Y. Et al. [13] presented the implementation of a traditional and polished strategy for medical tomography. Their research condenses the process to illustrate image definition restrictions via various imaging algorithms. X-ray produces 2D films of a human. Then, fluoroscopy detects the active organs. A patient is scanned all over the body area through a revolving x-ray tube in a CT scanner. They enhance the image to make the image standard better and perceivable through its program. Secondly, they used the image segmentation technique to make the image more analyzable and interpret preserving its quality. Thirdly, they convert them into black and white. Later, some types of edge detection techniques were used among them Robert kernel [14] and Prewitt kernel function are mentioned. It is concluded with various kinds of image processing approaches such as Segmentation and Thresholding.

S. I. Ayon Et al. [15] in their research, did a comparison between a number of computational intelligence techniques to predict CAD. They achieved a remarkable accuracy of 98.15%. Additionally, the accuracy of 98.67% 98.01% can be obtained with sensitivity and precision respectively. Firstly, they check the dataset to examine any missing values. Missing values can be handled by fully ignoring or replacing them with numerical values. In this paper, mean values were placed where values were missing. Then, they made division the data into two ways. The confusion ma-

trix visualizes the performance of computational intelligence techniques. Secondly, they applied all the techniques. Through their model, they achieved an accuracy of 98.15%.

P. Mirunalini Et al. [24] had successful research on identifying coronary arteries in a more efficient process. Conventionally, to diagnose a coronary artery thoroughly a surgical procedure is used. It is also a procedure to detect stenosis and other CAD. However, as part of their research, they devised a new model for comprehensively examining a coronary artery without the need for surgery. Here, they used 2D CTA (Computed Tomography Angiography) images and reconstructed them into 3D images. Firstly, an image of 150-200 slices is generated from CTA which are sorted to find coronary artery blocks as all slices do not contain artery information. CNN was used to create the feature map and then RNN was used to generate sequence information. The feature map of the input image is extracted by CNN and passed to the RNN to process the sequence information. Because the curvature of the coronary artery varies from slice to slice, a U-Net design is employed to segment it. They used a 3D image construction algorithm MIP (Maximum Intensity Projection) to construct a 3D image for the coronary artery. To test the validity of the result, SSIM (Structure Similarity Index Metrics) is used to compare the result images for every 10-degree angle. For all rotation angles, the system provides an average of 83-85 percent of SSIM values. The value may be enhanced even further by attaining more IOU metric value. This technique may also be used to analyze and quantify the severity of stenosis.

Another research by John S. Et al. [25] proposed a system claiming to be the most inexpensive, simple, and noninvasive method to detect coronary artery blockage. In their research, they used acoustic sound signals produced by turbulent blood flow to determine coronary artery blockage. It is a very simple non-invasive procedure to detect coronary artery blockage. Firstly, as input, we require the sound input by specific microphones generated by the blood flow through the arteries. Then process the sound input to generate a graph by signal processing technique. Different types of cardiac microphones were used to collect data. The collected data was amplified and filtered before converting the sound to digital signals. The whole process was based on two important components: the microphone and signal processing. By phonocardiogram method, they represented the graphical data produced by the activity of the blood flow and functions of the heart. Using signal processing methods like a diastolic window the generated graph was analyzed. Next, using feature detection algorithms like the Non-Spectral Technique, Zero Tracking, Time-Frequency, and Spectral-based method further analysis of the data was done to reach the conclusion. In conclusion, the results of the research model were found to be not promising as the model produced diverse results varying for different patients.

In research [26], they introduced a system that automatically detects lesions in cardiac coronary angiography. It was based on deep learning techniques. They created a model using a convolutional neural network and advanced building blocks such as CReLU, Inception, and other advanced building blocks. Following their testing, the CALD-Net was able to accurately recognize the stenosis lesion, with an 88% recall rate, finding the stenosis lesion that clinicians miss. Furthermore, CALD-Net was

used to detect various types of lesions and other technology to discriminate various types of coronary arteries in order to determine the SYNTAX score without the need for people's interaction.

In research by Wen J. Et al. [27] they introduce a method that is a systematic review of the test merit of MSCT angiography for coronary artery disease detection. MSCT angiography was differentiated from coronary angiogram in terms of symptomatic value at the segment and patient levels. Set side by side with four and Sixteen slice scanners, diagnostic correctness of MSCT angiography in estimating components was particularly enhanced with 64-slice scanners. In conclusion, their systematic analysis showed that MSCT angiogram offers the possibility to identify CAD with maximum accuracy. The latest 64-slice CT has greatly enhanced MSCT angiography diagnostic performance, resulting in high quantitative diagnostic fidelity. The spatial resolution of 16-slice CT was low, making quantitative measurement of coronary artery stenosis challenging.

In the research, X. Zhanchao Et al. proposed a robust method by using deep learning architectures with convolutional networks for main vessel segmentation. On a Clinical dataset composed of 3200 X-ray angiography images gathered from 1118 patients, four deep learning models based on Net architecture are evaluated. The average Pre, Re, and F1 for main vessel segmentation in the entire experiment data utilizing Pre, Re, and F1 scores as evaluation metrics are respectively 0.901, 0.898, and 0.900. The photos had a high F1 score which is greater than 0.8 (89.8%) of the cases. The author in their deep learning technique found out that the vessels could be separated in real-time with a more optimized execution for the major vascular segmentation XRA images, thus simplifying the online diagnosis of smart medicine. The robust method by X. Zhanchao Et al. is quite convincing as the existing methods had difficulty in finding the coronary artery structure in XRA images.[31]

K. Jihoon Et al. in another research also proposed a robust method using a deep learning model with the convolutional network for major vessel segmentation. Deep learning networks successfully identified and segmented the major arteries in X-ray coronary angiography when they were tested on angiographic pictures of 3302 diseased major vessels from 2402 patients. The most famous of the photos (93.7%) had high F1 scores which are greater than 0.8, with the average F1 score coming at 0.917. Having deep connections, the narrowest portion of the stenosis was clearly captured. For such an external dataset with various image features, the robust prediction was validated. K. Jihoon in their method showed that the prediction probably is finished in real-time with little picture pre-processing for major vascular segmentation.[32]

Chapter 3

Methodology

3.1 Architectures of Proposed Systems

The architecture of the proposed system diagram in figure 1 below shows an overview of each step to train, test, and validate our models. First of all, we collected our data sets of Angiogram images. Then we completed data pre-processing through Data splitting, normalization, resizing, and data labeling. After finishing pre-processing, we splitted our data set in a 7:3 ratio. 70% of the data set was used for training our model and 30% was used for testing. Next, we divided our data set into two classifications based on machine learning, one for Binary classification and another for Multiclass classification. Then, through several neural network model architectures like ResNet50, VGG16, VGG19, Inception V3, Densenet121, etc., we trained our model. After that, we did a comparison and found the validation accuracy of our model. From the comparison, we selected some top models that resulted in the highest accuracy and add them to get more precise results. Then, we applied the Ensemble learning model to our results from the top 3 highest accuracy gained models to comprehend and trust the results and output of our model. In the end, we came to a conclusion through the results we got from our system.

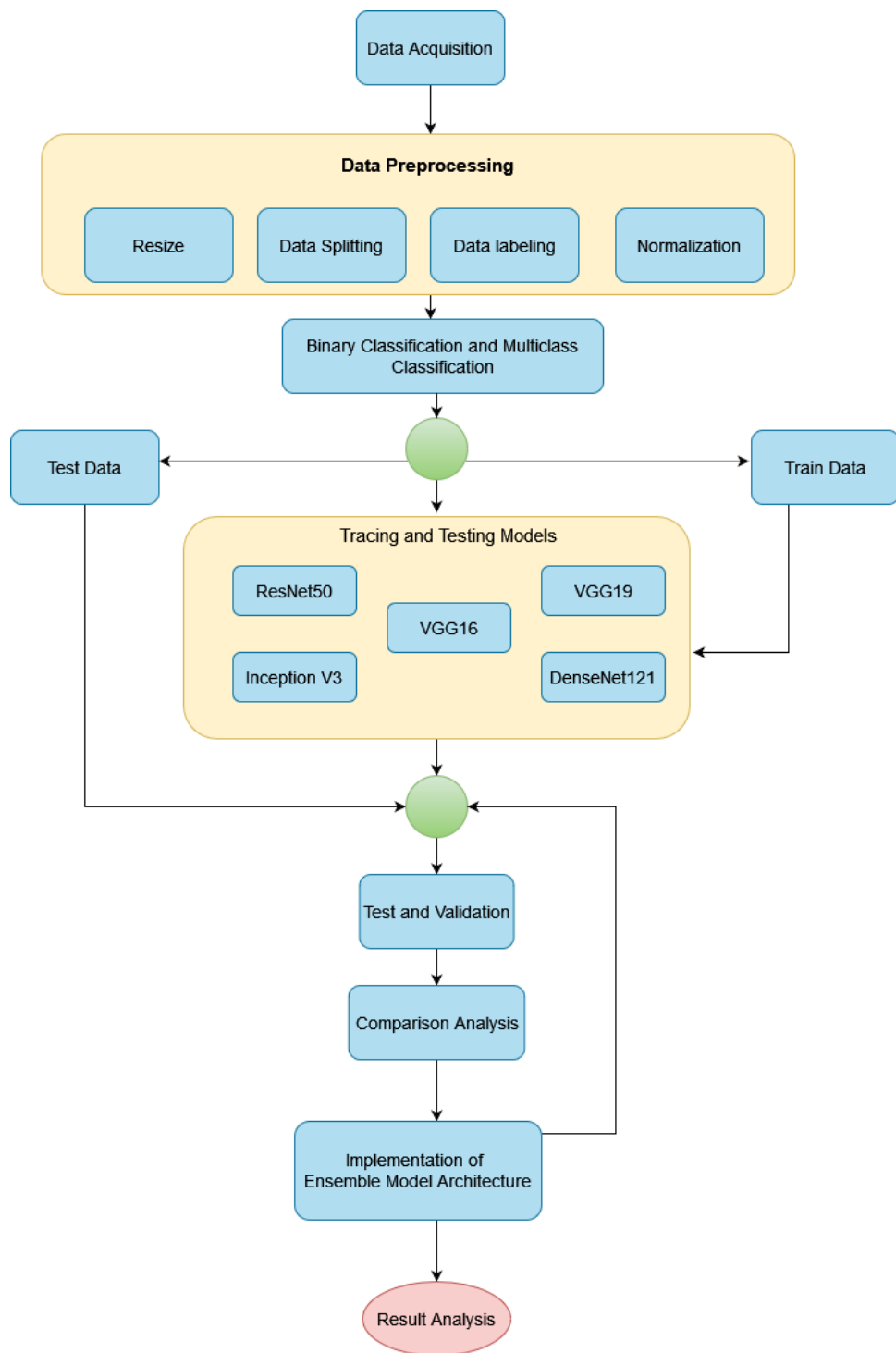


Figure 3.1: Proposed Architecture System Diagram

Binary classification issues can be effectively handled to a significant extent using Deep Learning Models. In order to acquire the greatest accuracy for our system, we divided our datasets into binary categories and trained them using deep learning models.

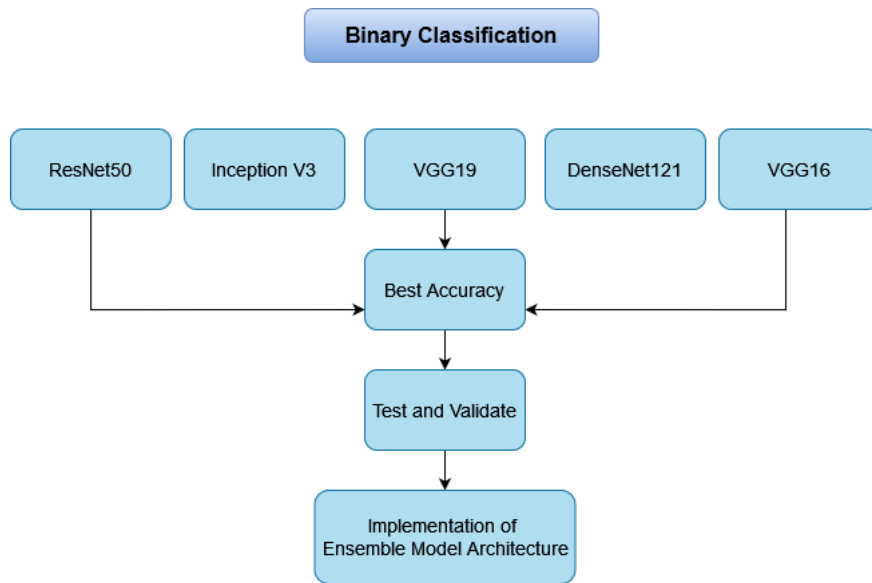


Figure 3.2: Binary Classification

When there are more than two classes in a dataset, it is quite difficult to analyse the data and determine the right accuracy. Multi-class classification in deep learning efficiently manages several classes and provides excellent accuracy.

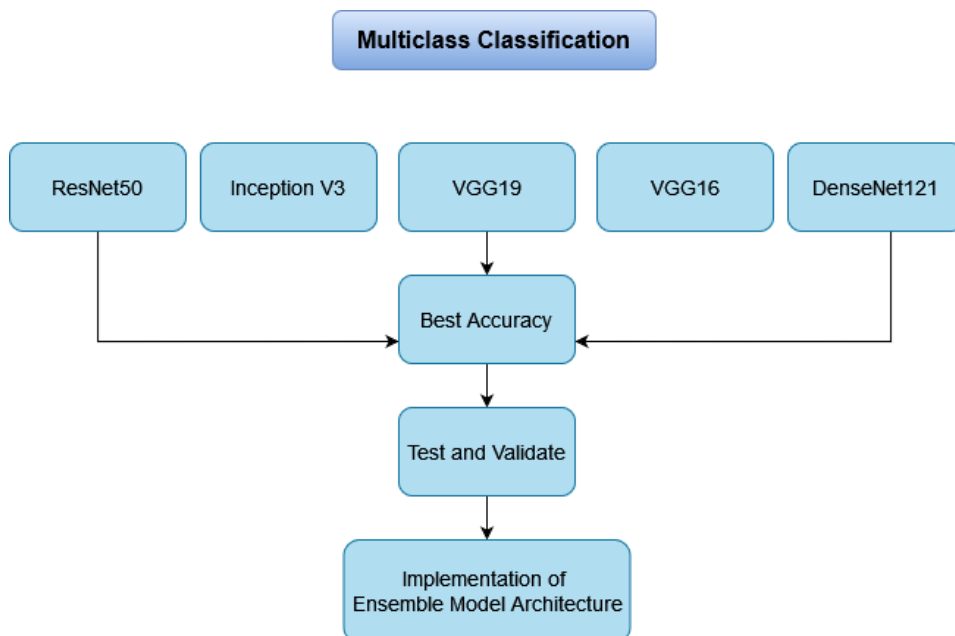


Figure 3.3: Multiclass Classification

3.2 Used Models and Architectures

3.2.1 ResNet50:

ResNet has significantly enhanced the performance of neural networks with more layers. ResNet allows you to train layers with hundreds or even thousands of them and still get great results. On ImageNet, it achieves 95.51% top-5 accuracy. [20] The

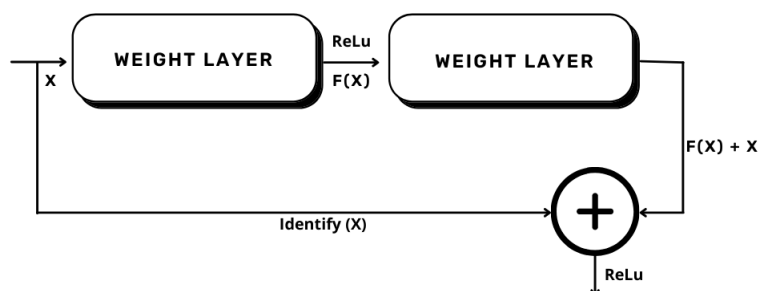


Figure 3.4: Residual Learning block

ResNet structure presented by Microsoft Research won first place in the ILSVRC 2015 competition. It has a structure similar to VGG in that the three-dimensional convolution is repeated three times. According to the number of layers, it is classified as ResNet-18, ResNet-34, ResNet-50, ResNet-101, ResNet-152, and so on. The input feature map is added to the output through a shortcut to the side of the two 14 convolution layers, which is commonly an identity shortcut. When the number of output feature maps doubles, a method of halving the width and length of the feature map is employed instead of pooling, and a convolution process with stride = 2 is utilized instead of pooling. ResNet-50 is used in this paper. When models have more than 50 feature maps, the bottleneck structure from the inception module is used to overlap the bottleneck residual block.

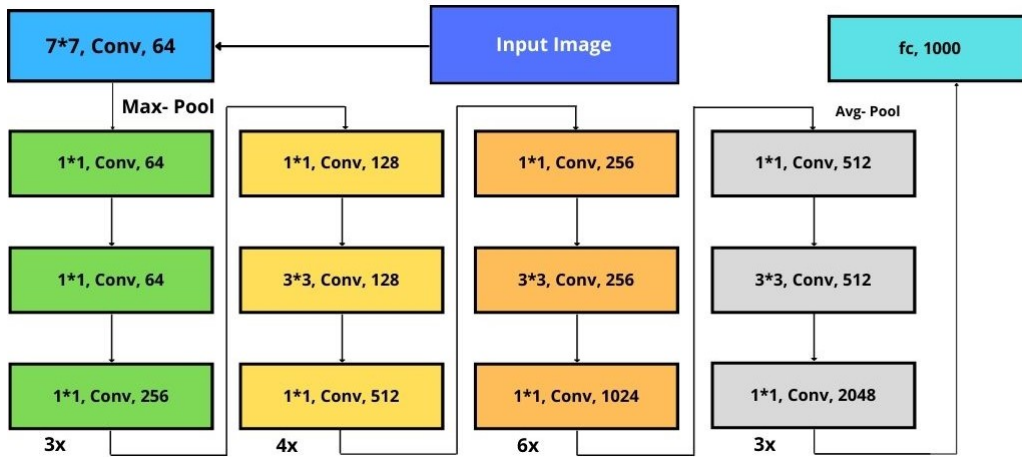


Figure 3.5: Internal Architecture of ResNet50

3.2.2 VGG16:

Convolutional neural network model VGG16, developed in 2014, is still regarded as one of the top models for classifying images. Convolutional neural networks are used as the network infrastructure in the successful image identification technique known as the VGG16 model. It has a unique network structure that seems to be simple to change. The VGG16 network consists of 22 maximum-pooling layers and 33 filters, with 16 layers made up of 5 blocks and 1 maximum-pooling layer each. Between these levels, the activation function of ReLU is utilized. Three completely linked layers follow, in which the majority of the network's parameters are held. Lastly, using a Softmax activation feature, the chances of each classification of pulmonary symptoms are determined. With a 3*3 size kernel, a 224*224*3 RGB image that has been passed through several evolutionary stages is used as the network input. The filters are measured in 2*2 measures and connected to two segments between the maximum-pooling layers.

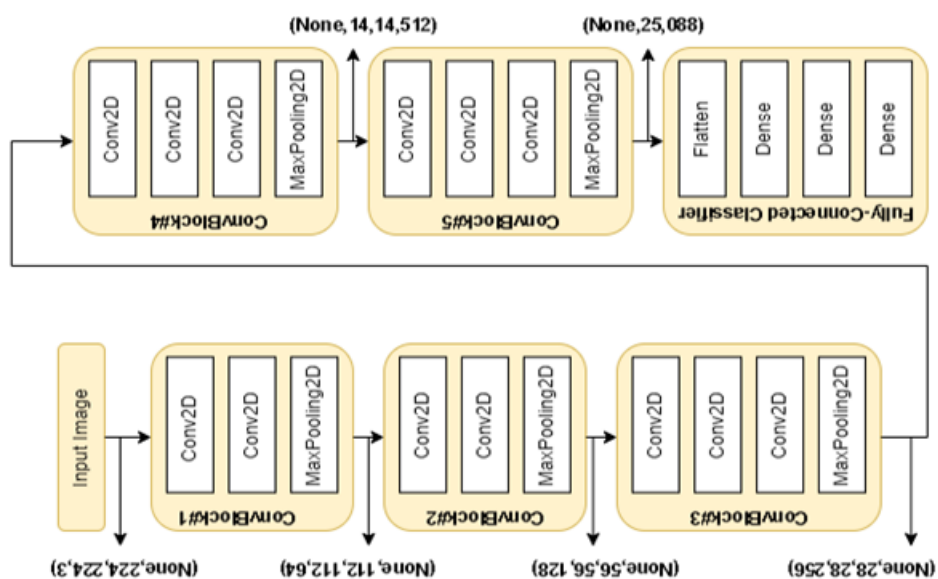


Figure 3.6: Internal Architecture of VGG16

3.2.3 VGG19:

Consisting of blocks where each block has 2-dimensional convolution and max pooling layer, VGG is an object or image recognition model. VGG performs best in managing large scale data. This is used for large-scale picture identification and has a top-five test accuracy of 92.7% in ImageNet. [20] The VGG Network is characterized by its simplicity because it has a 3-dimensional convolution layer and two-dimensional max pooling layers. Max pooling is used to reduce the volume size. In the pre training smaller networks converged and then utilized as larger, deeper networks. Pre training is time consuming while making the logical sense. There is one more drawback in VGGNet which is that the network architecture weights themselves are quite large (In terms of disk/bandwidth). Because of the depth and number of fully connected nodes VGG19 is over 574 MB and for that reason VGG is arduous work. [28]



Figure 3.7: Internal Architecture of VGG19

3.2.4 Inception V3:

The Inception model is also a convolutional neural network that aids in the classification of various objects on photographs. There are three different versions. Version 3 is the most popular since it provides the highest accuracy. On ImageNet, it achieves 93.3% top-5 accuracy and is substantially faster than VGG. [21] The objective of inception is to operate as a multi-level feature extractor by computing 1,3- and 5-dimension convolution within the same network module. with the output of these filters being stacked along the channel dimension before being sent into the next layer. Inception-v3 is a more advanced version of the well-known GoogLeNet network, which has demonstrated strong classification performance in a variety of biological applications employing transfer learning. Inception-v3 suggested an inception model that concatenates multiple different sized convolutional filters into a new filter, similar to GoogLeNet. The weights for Inception V3 are 96MB, which is less than VGG and ResNet. The number of parameters that must be taught is reduced as a result of this architecture, as is the computing complexity. It employs Label Smoothing, factorized 7-dimension convolutions, and an auxiliary classifier, all of which are improvements over previous Inception members.

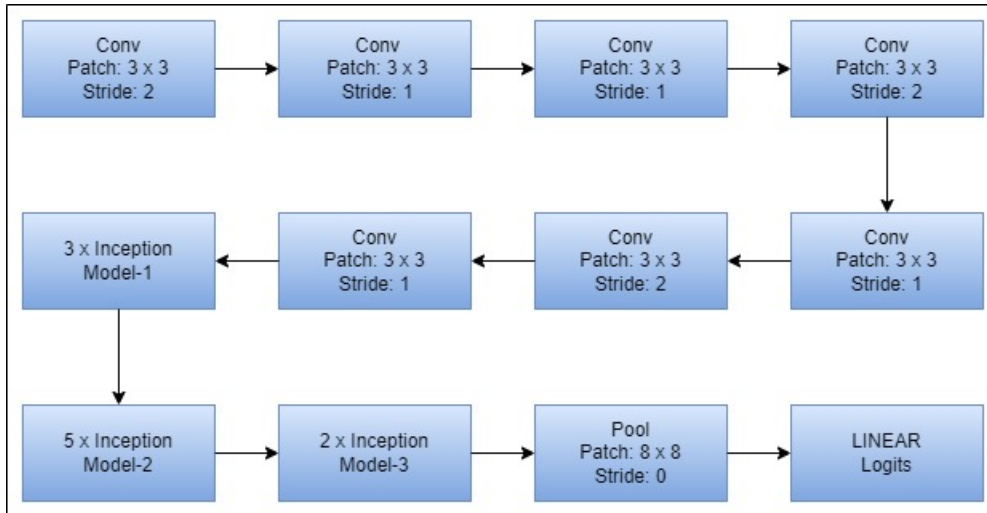


Figure 3.8: Internal Architecture of Inception V3

3.2.5 DenseNet121:

DenseNet uses a specific smaller connection between layers using blocks connected to each other to create a feature map of the same size. It is a type of CNN. The network creates relatively shorter and smaller channels. As a result, It is more efficient in terms of computing and memory. DenseNet can obtain a level of accuracy of 94.48%. [23] According to recent research, convolutional networks can be significantly deeper, more precise, and easier to train if they have shorter connections between layers that are near to the input and ones that are close to the output. DenseNets offer a variety of significant benefits, including the elimination of the vanishing-gradient issue, improved feature propagation, encouraged feature reuse and substantially fewer parameters. DenseNets achieve significant improvements over the state-of-the-art despite requiring less memory and processing power to attain great performance.

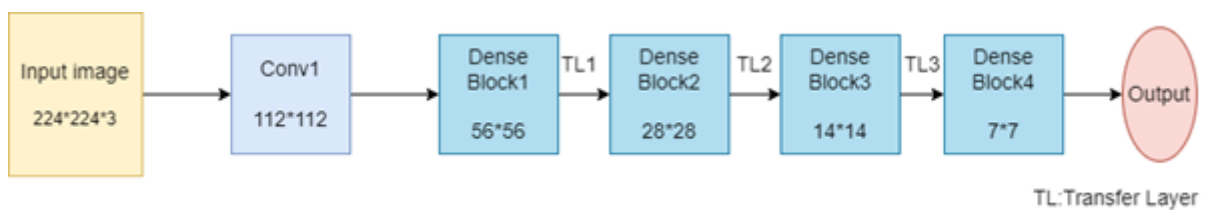


Figure 3.9: Internal Architecture of DenseNet121

3.2.6 Ensemble Model:

Ensembles are multi-layer predictive models that combine forecasts from multiple models to provide a single prediction. The ensemble participants' predictions can be aggregated using statistics like mean, median, mode or more complicated techniques to define the amount and in what circumstances to consider individual participants. On a predictive modeling task, ensembles have been used to improve the prediction performance of individual prediction models. This is achieved by introducing bias into the system, which lowers the prediction error's variance component. Greater resilience or consistency in the standard outcomes of an architecture is a key benefit of ensemble methods. The effectiveness of the bias and variance of a model are related. Variance and bias are mainly errors from a model. Sometimes reducing bias is as simple as increasing variance. The primary benefit of using ensembles is to boost predictive accuracy by lowering the variance features of prediction error.

3.3 Convolutional Layer

Convolutional Layer is the basic component of a Convolutional Neural Network. This network works best for two-dimensional data. This layer is made of convolutional filters that convert two dimensional images to three-dimensional images. In this layer learning occurs rapidly by the model. CNN is a multilayer perceptron. It has the ability to distinguish visual patterns in raw image pixels. [33]

3.3.1 Activation Function

Gross Inputs are the significant units of a neural network structure. First, these gross inputs are processed. Then, the inputs are transformed into a final output called unit activation using an activation function. The output of a network layer can range from negative infinity to positive infinity. [34]

Rectified Linear Unit(ReLU)

ReLU is a non-linear activation function [35] which is used widely in neural networks. It is more efficient than other functions. In ReLU, all neurons are not activated simultaneously. For this reason it works more efficiently in comparison to other activation functions. Moreover, in the back-propagation stage of neural network training, weights and biases remain unmodified because the value of the gradient is 0.

$$f(x) = \max(0, x) \tag{3.1}$$

Softmax

Multiple sigmoid curves were assembled to obtain a Softmax function. The outputs which it provides, vary from 0 to 1. Therefore, it is used as probabilities of the data points whether it is in a certain class or not.[36] The Softmax function gave

the solution to the issues with multi-class. For certain classes, probability returns a function

$$f(x) = \frac{e^{x_i}}{\sum_{n=1}^k e^{x_i}} \quad (3.2)$$

3.4 Confusion Matrix

A Confusion matrix is a N x N matrix used to assess the effectiveness of a classification model, where N is the number of target classes. The matrix compares the actual goal values to the machine learning model's predictions. A confusion matrix is a table that shows which classifications are valid and which are erroneous. To indicate the classifier's performance, a variety of metrics are constructed based on the confusion matrix's results. The following four outcomes are represented by values in a confusion matrix:

- TP (True Positive)
- TN (True Negative)
- FP (False Positive)
- FN (False Negative)

The number of correctly classified samples to the total quantity of data is used to determine classification accuracy.

$$Accuracy = \frac{Total\ Number\ of\ correctly\ classified\ samples}{Total\ Data} \quad (3.3)$$

The ability of a classification system to detect true positive results is demonstrated by recall.

$$Recall = \frac{TP}{TP + FN} \quad (3.4)$$

The capacity of a classification to find only true positives is measured by precision.

$$Precision = \frac{TP}{TP + FP} \quad (3.5)$$

The F1 ratio is obtained by taking the harmonic average of these two metrics.

$$F1\ ratio = \frac{2 * Precision * Recall}{Precision + Recall} \quad (3.6)$$

Classification accuracy may be used to assess performance as long as the dataset contains an equal number of samples from each class.

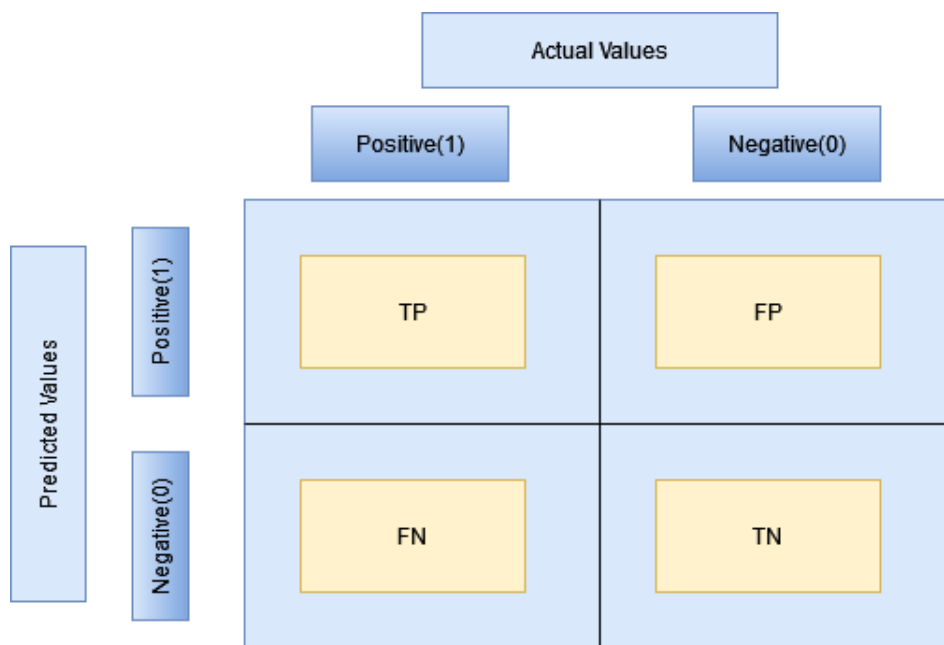


Figure 3.10: Confusion Matrix

Chapter 4

Implementation

4.1 Dataset

Our dataset consists of 2,151 Angiogram images of the human heart of both types - blocked and unblocked coronary artery in random order.

4.1.1 Source

Coronary Angiography Print Images of heart dataset from Kaggle Image. Library Link: <https://www.kaggle.com/datasets/turkertuncer/coronary-angiography-print>

4.1.2 Data Classification

We classified our dataset into two different classes.

- Binary Classification
- Multiclass Classification

Binary Classification: There are human heart images affected by a coronary artery blockage and a human heart with no blockage. As a result, we represented our data using a binary classifier. In our dataset, the “Class” attribute defines two categories of data in binary representation. In the class attribute, 0 represents the number of unaffected hearts which is labelled as ‘No block’ and 1 represents the number of hearts with coronary artery blockage labelled by ‘Block’.

Multiclass Classification: In this segment, we classified our dataset into more variables narrowing down the dataset into different classes. We classified the data to 5 Classes ‘LAD,’ ‘LCX’, ‘RCA’, ‘Multiple’ and ‘No block’. The angiogram images of the dataset of heart are segmented to identify the coronary arteries for the detection of coronary artery blockage. This can be inferred that the images with narrowed arteries are the blocked one and the rest are with no block.

In the above figure, the images represent the dataset of CTA Images of heart which are segmented to identify the coronary arteries for the detection of coronary artery blockage. This can be inferred that the Images with narrowed artery are the blocked or narrowed artery.

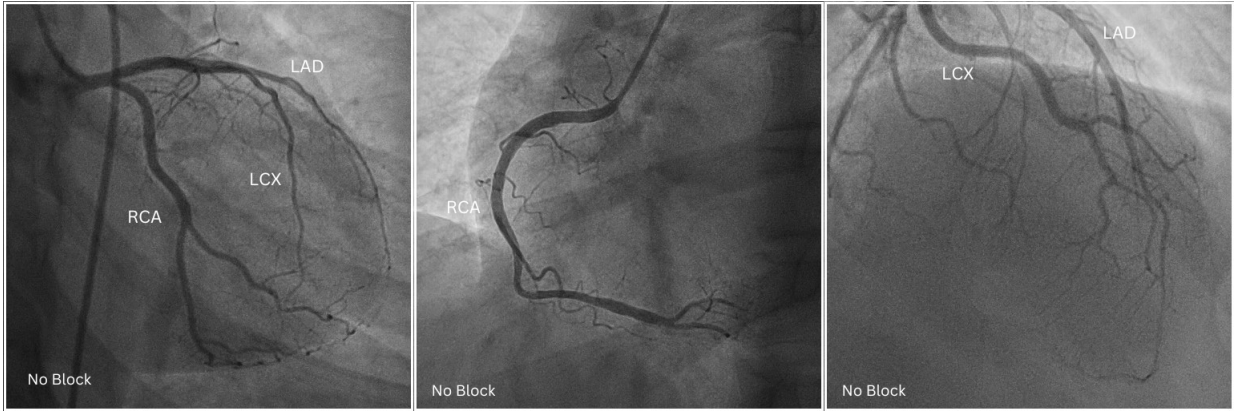


Figure 4.1: Healthy Heart Angiogram Image

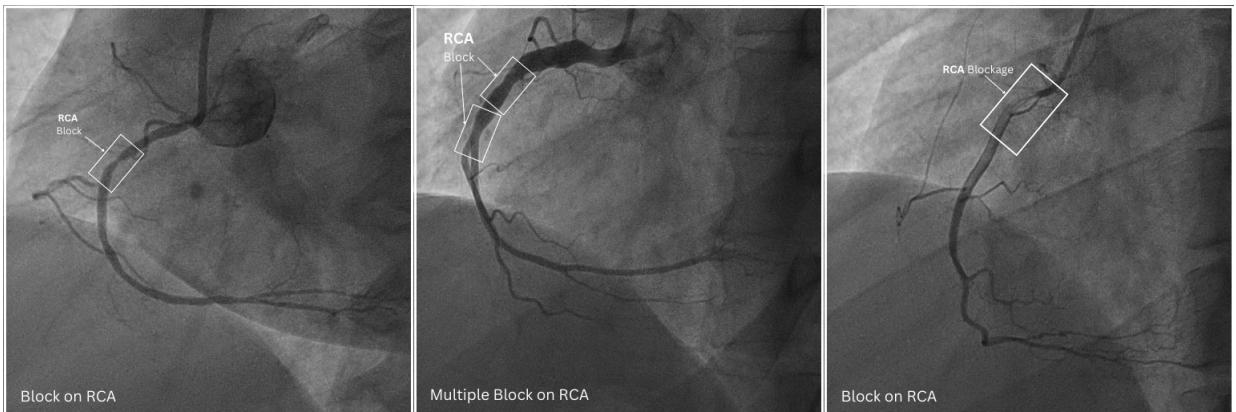


Figure 4.2: Blocked Heart Angiogram Image

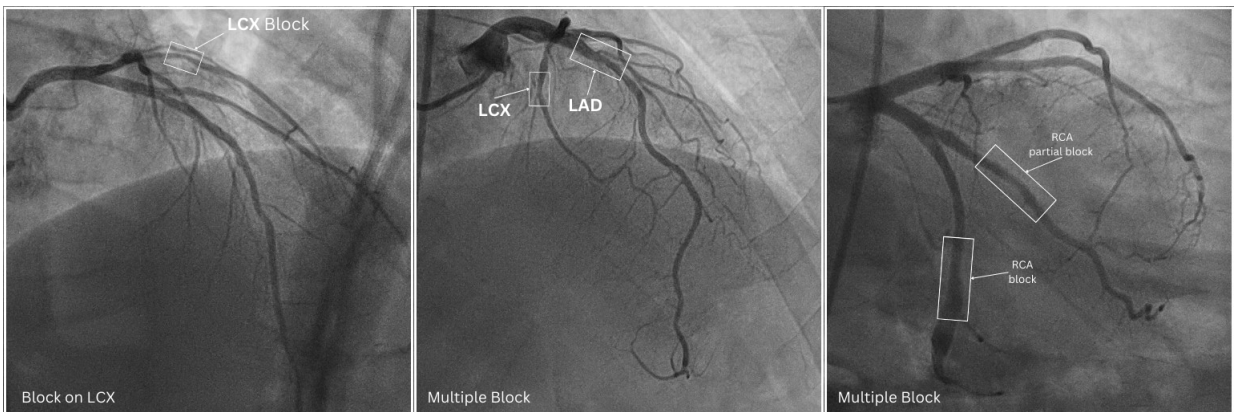


Figure 4.3: Blocked Heart Angiogram Image

4.2 Data Preprocessing

4.2.1 Data Labels

Firstly, we classified our dataset into two different labels which are ‘Block’ and ‘No block’. Which is human heart images affected by a coronary artery blockage and a human heart with no blockage in their arteries. And used this for the Binary classification. Moreover, the dataset was again classified into 5 classes according to blockage in the heart arteries. The heart arteries are classified into 3 segments

‘LAD’, ‘LCX’, ‘RCA’, these 3, another 1 class for multiple blockage ‘Multiple’ and lastly 1 class for no blockage ‘No block’. These labelling of angiogram heart images was done through two very experienced doctors.

4.2.2 Image Resizing

We used convolutional neural network model architectures like VGG16, VGG19, ResNet50 and other models in our research. These models fit best with the input size for 224x224 pixels. Because they have 224 nodes horizontally and 224 nodes vertically. So to resize the image we will use the TensorFlow.

4.2.3 Data Splitting

In our research to split the data into test and validation, we have used split-folders. Split-folders are a very handy algorithm to split data into test train validation for image datasets. It shuffles the data very effectively. It randomizes the oversampling of imbalanced datasets.

4.2.4 Normalization

Normalization is used to remove information from the less important pictures and reduce data repetition. For normalization, the PCA (Principal Component Analysis) method was utilized. A vast data variable is reduced to a tiny data variable using PCA, preserving the majority of the data [29]. To normalize the Coronary Artery angiogram images projection, Eigen flat fields are developed and combined. After that, dynamic at fields reduces the systematic mistakes in projection intensity normalization [30]. The Keras ImageDataGenerator class was used to perform this challenge. Normalization techniques confine data to a scale of 0-1 scale by changing re-scaled input to a ratio that may be multiplied by each pixel.

Chapter 5

Result and Analysis

5.1 Result and Analysis

In this study, we have done the analysis in two ways. One is Binary classification where it has two classes: Block and No block. And another is Multiclass classification, where we have divided the datas into 5 classes. The classes are LAD, LCX, RCA, Multiple and No block. For the performance analysis we have used various performance metrics like validation accuracy, precision, recall, F1 score along with confusion matrix and graphs.

5.2 Binary Classification

5.2.1 ResNet50

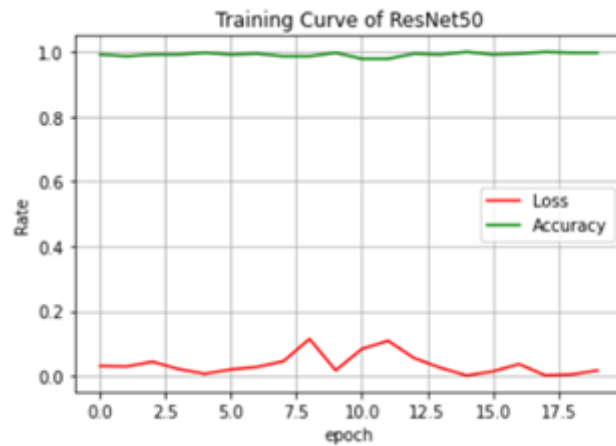


Figure 5.1: Training curve(s) of ResNet50 architecture

The accuracy of training curves remained constant throughout the ResNet50 model's training phase and was close to 1.0. When it came to the loss curve, the rate of change was frequently under or close to 0.2.

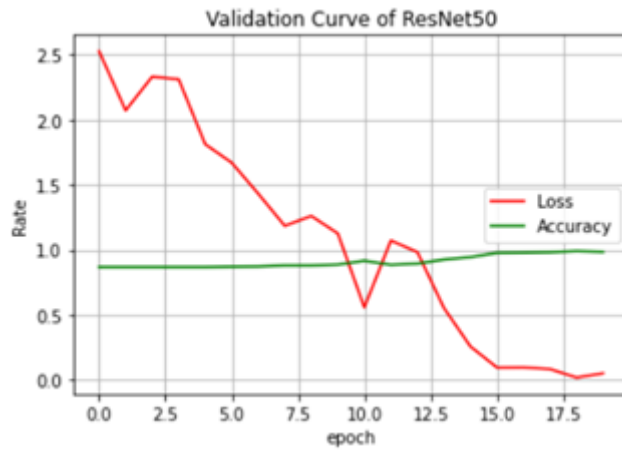


Figure 5.2: Validation curve(s) of ResNet50 architecture

Regarding the ResNet50 model's validation curve, the accuracy rate stays close to 1.0 from epoch 0 to epoch 20. On the other hand, at epoch 30, the loss curve gradually decreased from 2.5 to close to 0.0.

5.2.2 VGG16

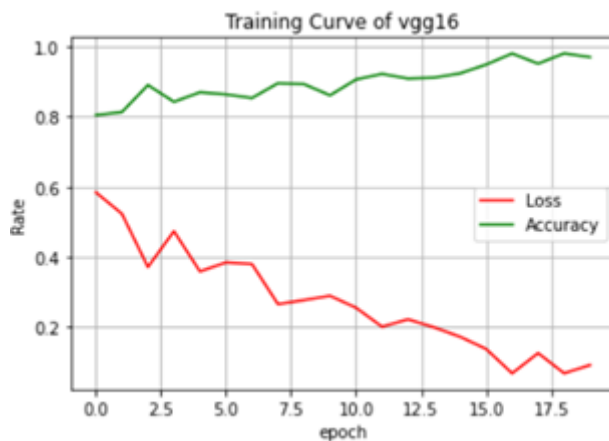


Figure 5.3: Training curve(s) of VGG16 architecture

The accuracy curve is rising at an increasing pace, as indicated by the VGG16 training curve. When compared to its nature after epoch 16, the rise was very apparent from epoch 0 to 16. In contrast to the accuracy curve, the loss curve displayed a rapid decline in change rate until 0.4. After that, the curve had a few minor spikes, although they weren't as obvious as they had been in the earlier instance.

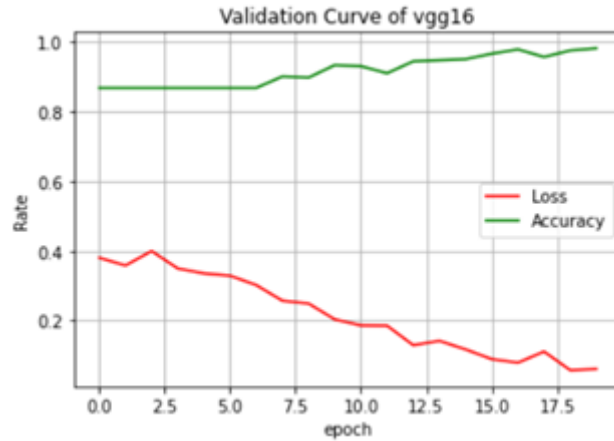


Figure 5.4: Validation curve(s) of VGG16 architecture

The accuracy curve stayed constant from epoch 0 to epoch 6, according to the aforementioned VGG16 validation curve, but the rate rose quickly and remained constant. In addition to the loss curve, from epoch 2 to epoch 11, the rate of change dramatically dropped from around 0.4 to 0.1. After that, there was little variation in the pace of change.

5.2.3 VGG19

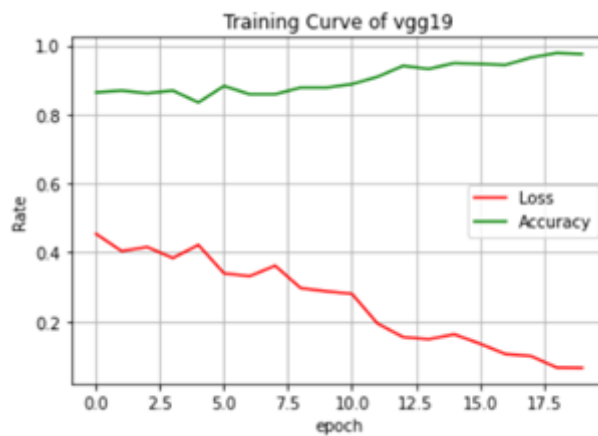


Figure 5.5: Training curve(s) of VGG119 architecture

Figure 5.2.5 shows that throughout training, accuracy stayed constant from epoch 0 to epoch 3, and after a brief decrease, the accuracy curve began to rise faster. As the rate of descent relatively increased, there were obvious alterations in the loss curve.

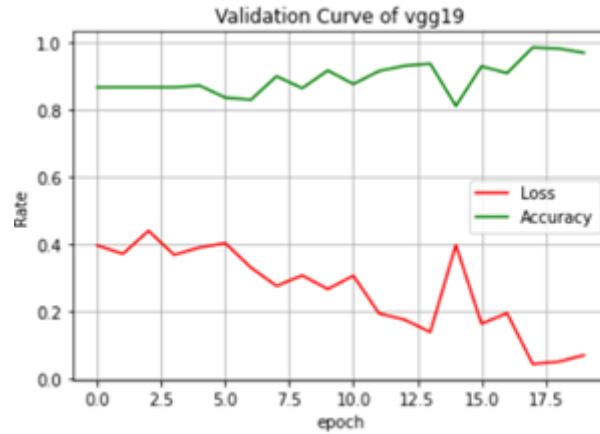


Figure 5.6: Validation curve(s) of VGG19 architecture

From epoch 0 to epoch 4, the VGG19 model’s accuracy for its validation curve remained unchanged. Comparing the subsequent scenario to the initial one, the rate of change was less apparent. The loss curve also saw substantial variations between epochs 0 and 13. After then, the curve had a few minor spikes, although they weren’t as prominent as they had been in the earlier instance.

5.2.4 Inception V3



Figure 5.7: Training curve(s) of Inception V3 architecture

The training curves for the Inception V3 model were created during the training phase and included both accuracy and loss curves. The accuracy curve’s rate remained constant around 1.0 after increasing until about epoch 15. On the other hand, until epoch 4, the rate of change of the loss curve substantially dropped.

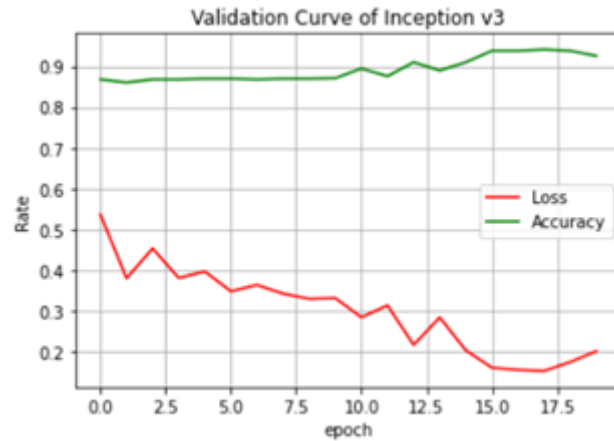


Figure 5.8: Validation curve(s) of Inception V3 architecture

Accuracy consistently approached 0.9 at the conclusion of epochs in the Inception V3 model’s validation curve. And from epoch 20 on, the loss curve steadily flattens out.

5.2.5 DenseNet121

Training curves for accuracy and loss were generated during the DenseNet121 model’s training phase. According to the graph, accuracy steadily climbed from 0.8 to 1.0 from epoch 0 to epoch 15 before remaining constant until epoch 20.



Figure 5.9: Training curve(s) of DenseNet121 architecture

Similar to the above, the loss curve gradually decreased from 0.7 to close to 0.0 at epoch 18 and remained constant. The accuracy of DenseNet121’s validation curve

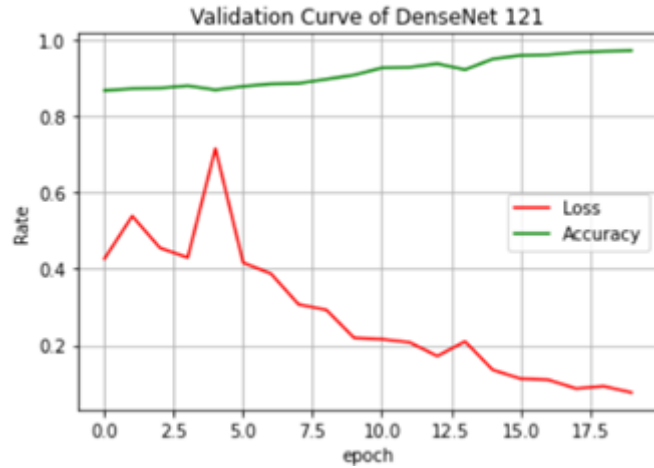


Figure 5.10: Validation curve(s) of DenseNet121 architecture

is rising steadily. The growth was quite observable from epoch 0 to epoch 11. For the loss curve, however, the rate of change fell repeatedly after a little fluctuation from epoch 4 to epoch 5.

5.2.6 Ensemble Model

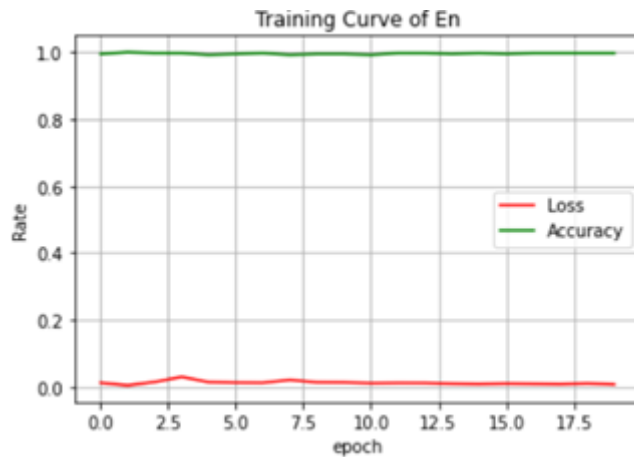


Figure 5.11: Training curve(s) of Ensemble Model architecture

The training curve of the ensemble model shows that the accuracy graph remained around 1.0 from epoch 0 to epoch 20. Again for the loss curve, it remained throughout except for epoch 3.

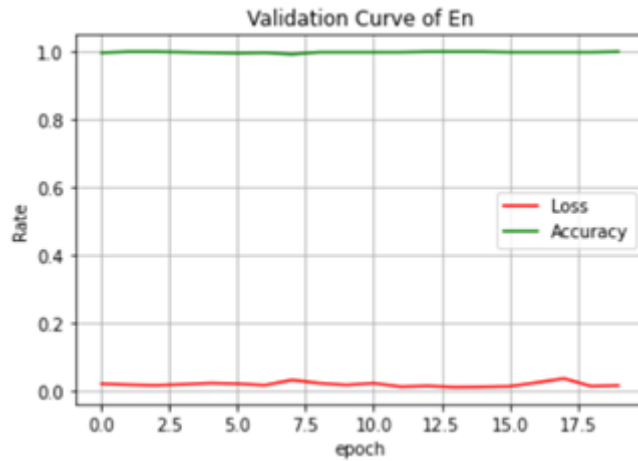


Figure 5.12: Validation curve(s) of Ensemble Model architecture

Regarding the ensemble model's validation curve, the accuracy rate stayed close to 1.0 from epoch 0 to epoch 50. The loss curve, on the other hand, had abrupt rises and falls, although the rate of rise did not exceed 0.1 for any of the epochs depicted above.

5.3 Multiclass Classification

5.3.1 ResNet50

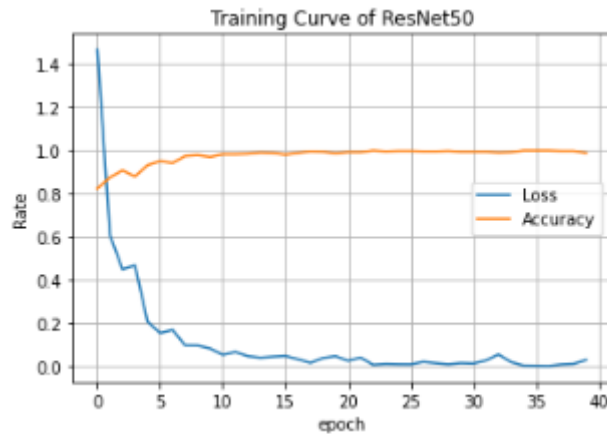


Figure 5.13: Training curve(s) of ResNet50 architecture

Throughout the ResNet50 model's training phase we have run 40 epochs, the training curves did not change much and were around 1.0. For the loss curve the rate of change was quite often but under or near 0.02.

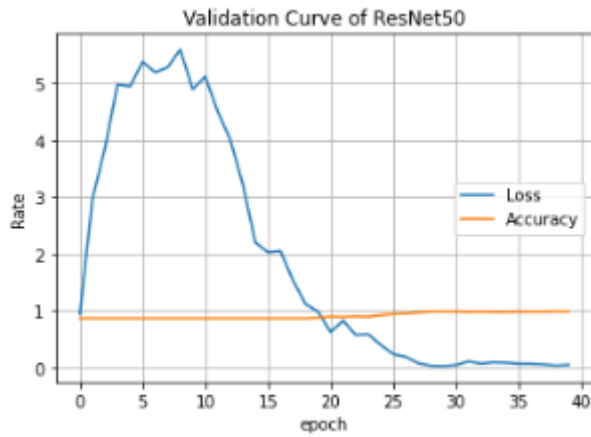


Figure 5.14: Validation curve(s) of ResNet50 architecture

Here in the ResNet50 model validation phase, the curve was steady and close to 1. But in the loss curve there was a huge change which lastly dropped nearly to 0.

5.3.2 VGG16

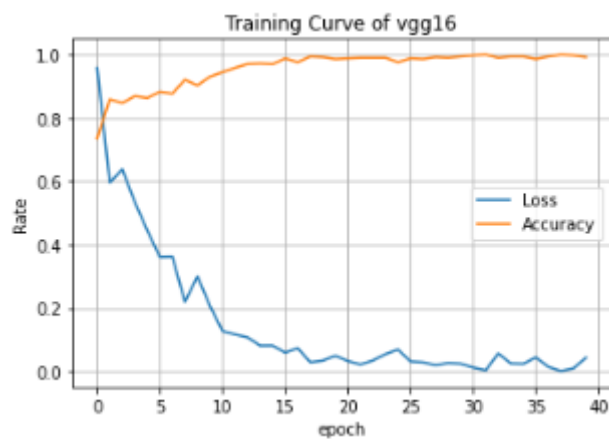


Figure 5.15: Training curve(s) of VGG16 architecture

In the VGG16 model's training phase, the training curve was around 1.0. For the loss curve the rate of change was quite often but under or near 0.04.

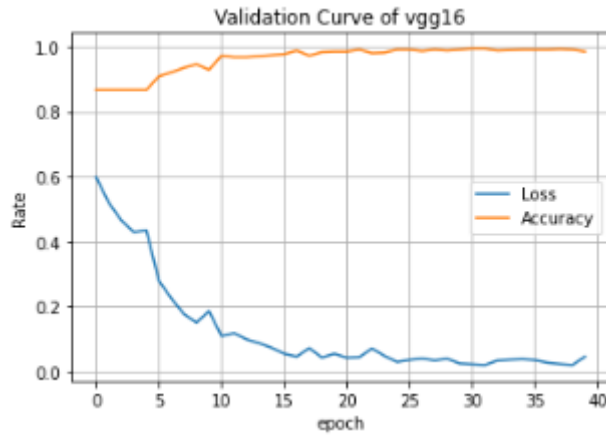


Figure 5.16: Validation curve(s) of VGG16 architecture

Here in the VGG16 model's validation phase, the curve was steady and close to 1. But in the loss curve there was a change which lastly dropped nearly to 0.04.

5.3.3 VGG19

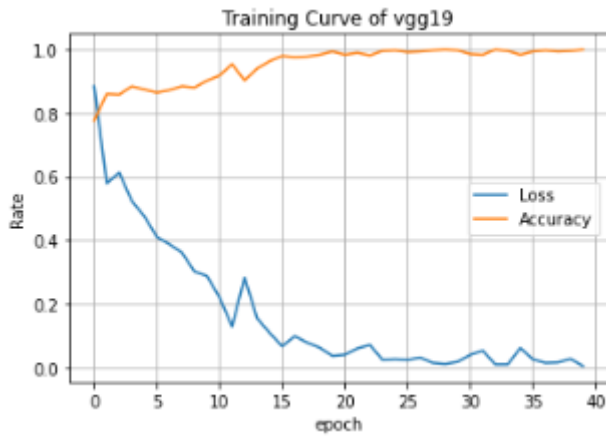


Figure 5.17: Training curve(s) of VGG19 architecture

From the figure 5.17 we can see in the training phase of VGG19 model, the accuracy curve had some change among the epochs and lastly in the 40th epochs it reached nearly to 1.0. And in the loss curve it eventually dropped close to 0.

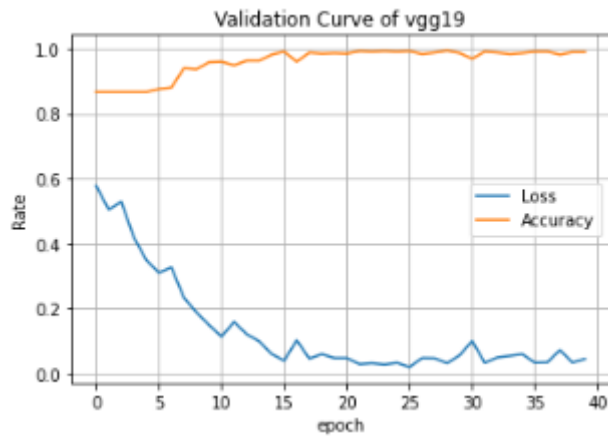


Figure 5.18: Validation curve(s) of VGG19 architecture

In the validation portion of VGG19 model, the accuracy curve was quite firm from epoch 16-40 it was close to 1.0. In the case of the loss curve the loss was between 0.6 to nearly 0.

5.3.4 Inception V3



Figure 5.19: Training curve(s) of Inception v3 architecture

In the Inception v3 model training phase, the accuracy curve stayed between 0.7 to nearly 1.0. And the loss curve fluctuated between 0.8 to 0.01.

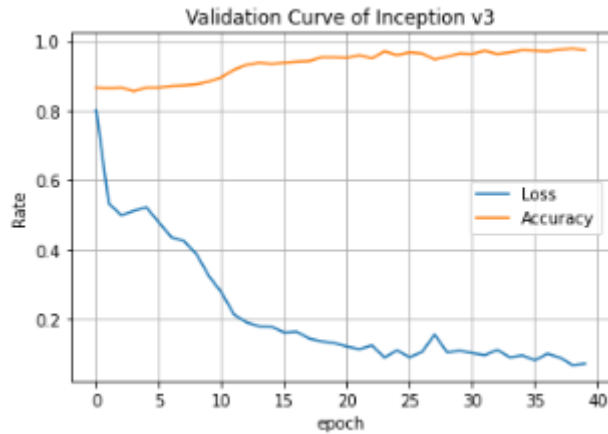


Figure 5.20: Validation curve(s) of Inception v3 architecture

In the validation curve of the Inception v3 model, the accuracy reached nearly to 1 at the end of the epochs. And the loss curve reached 0.06 at the end .

5.3.5 DenseNet121

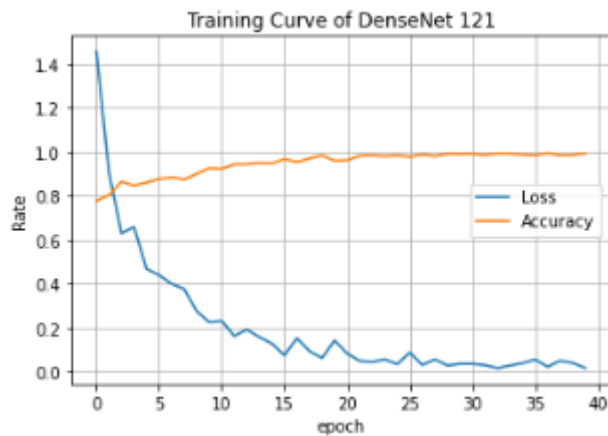


Figure 5.21: Training curve(s) of DenseNet121 architecture

In the illustration of the Densenet121 model training phase, the accuracy was close to 1.0 from epoch 20 to onwards. Besides in the loss curve at first it was very unsteady but gradually it reached nearly to 0.

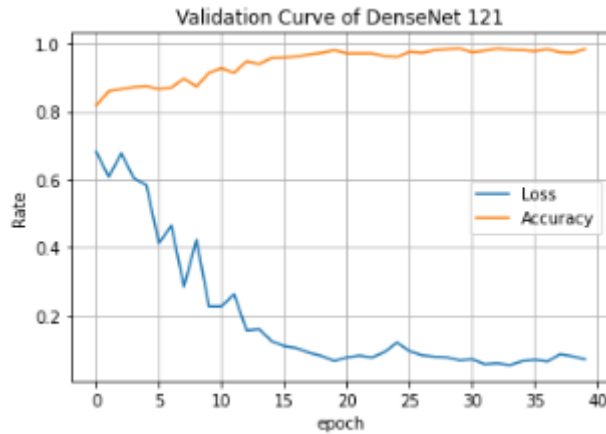


Figure 5.22: Validation curve(s) of DenseNet121 architecture

Again, in the illustration of the DenseNet121 model validation phase, the accuracy curve improved moderately, finishing close to 1.0. On the other hand, the loss was fluctuating and at the end of the 40 epoch it reached nearly to 0.06.

5.3.6 Ensemble Model

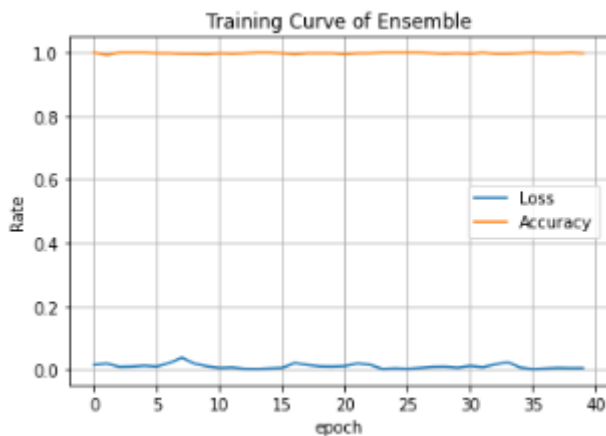


Figure 5.23: Training curve(s) of Ensemble model architecture

In the figure 5.23 the Ensemble model training curve is illustrated, here the accuracy curve was very firm and from the beginning to the end of epoch its curve is close to 1.0. Similarly in the loss curve the curve was nearly to 0.

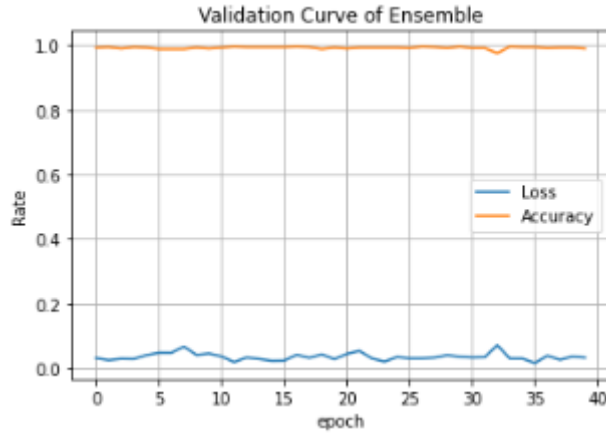


Figure 5.24: Validation curve(s) of Ensemble model architecture

In the case of the validation curve of the Ensemble model, the accuracy curve was quite balanced and stayed nearly to 1.0 and in the loss curve there was some up and down of the curve and it stayed under 0.04.

5.4 Confusion Matrix

Confusion matrix helps to understand the performance of a model architecture in a very efficient and easy way. This matrix gives a good understanding of the accurate and error portion of a model. In our study we have done, confusion matrix for both Binary classification and Multiclass Classification.

5.4.1 Binary Classification

ResNet50

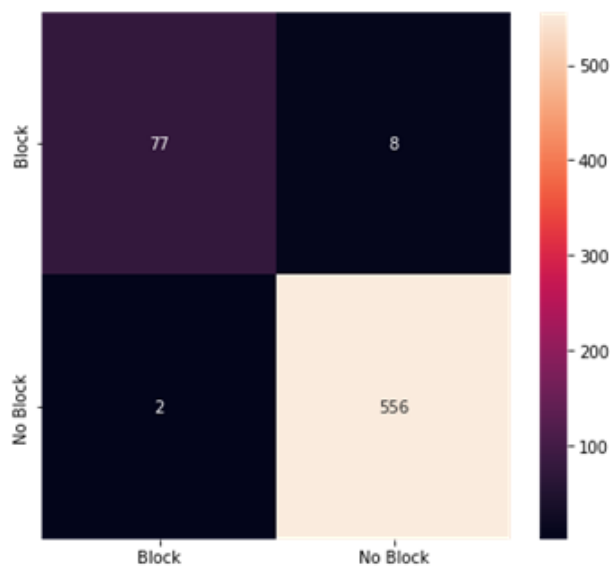


Figure 5.25: Confusion Matrix of ResNet50

According to the ResNet50 confusion matrix above, 556 images were classified by No Block. However, the algorithm incorrectly categorised 2 of the affected images as Block in the process. However, the system correctly categorised 77 images as Block, but the system incorrectly classified 8 images which is an error.

VGG16

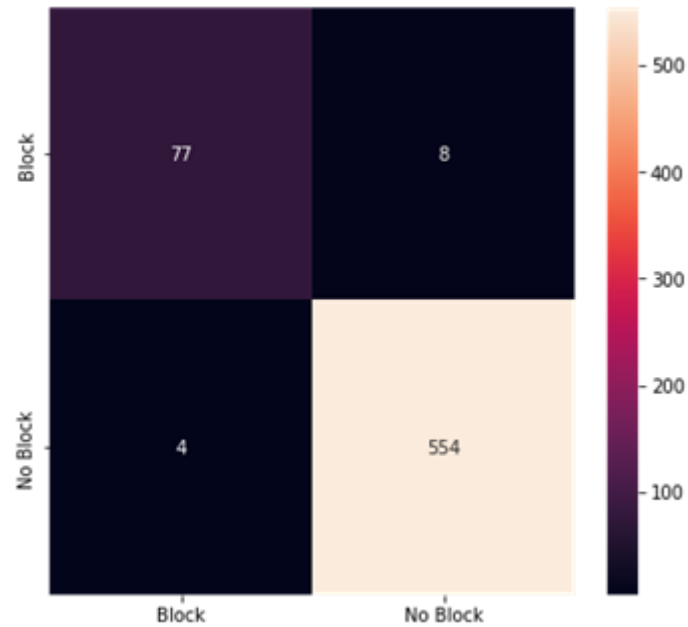


Figure 5.26: Confusion Matrix of VGG16

According to the VGG16 confusion matrix above, 554 images were classified by No Block. However, the algorithm incorrectly categorised 4 of the affected images as Block in the process. However, the system correctly categorised 77 images as Block, but the system incorrectly classified 8 images which is an error.

VGG19

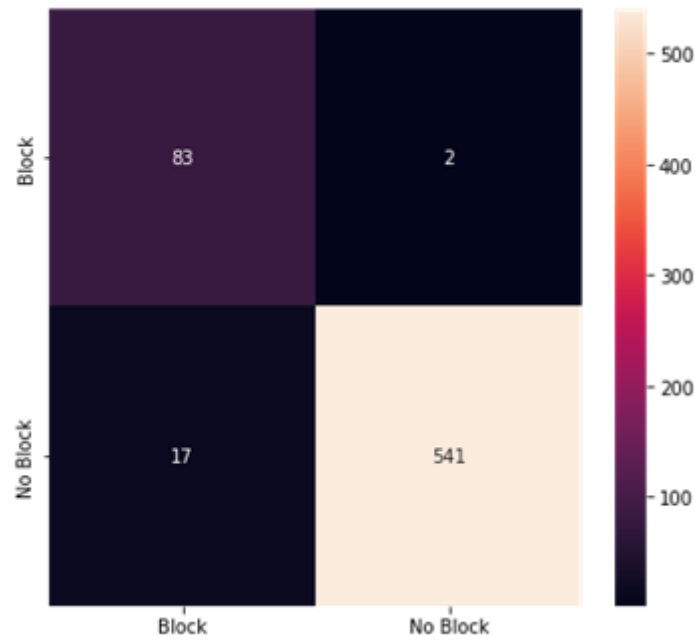


Figure 5.27: Confusion Matrix of VGG19

According to the VGG19 confusion matrix above, 541 images were classified by No Block. However, the algorithm incorrectly categorised 17 of the affected images as Block in the process. However, the system correctly categorised 83 images as Block, but the system incorrectly classified 2 images which is an error.

Inception V3

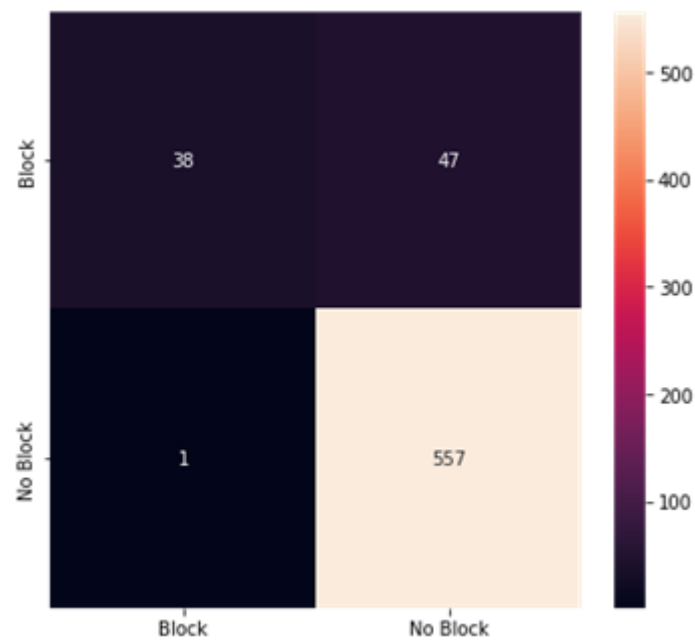


Figure 5.28: Confusion Matrix of Inception V3

According to the InceptionV3 confusion matrix above, 557 images were classified by No Block. However, the algorithm incorrectly categorised 1 of the affected images as Block in the process. However, the system correctly categorised 38 images as Block, but the system incorrectly classified 2 images which is an error.

DenseNet121

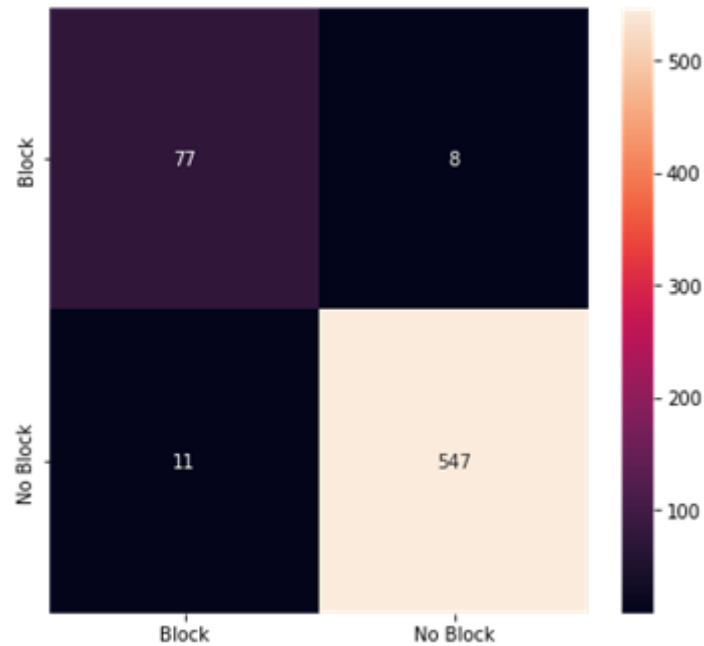


Figure 5.29: Confusion Matrix of DenseNet121

According to the DenseNet121 confusion matrix above, 547 images were classified by No Block. However, the algorithm incorrectly categorised 11 of the affected images as Block in the process. However, the system correctly categorised 77 images as Block, but the system incorrectly classified 8 images which is an error.

Ensemble Model

According to the Ensemble Model confusion matrix above, 557 images were classified by No Block. However, the algorithm incorrectly categorised 1 of the affected images as Block in the process. However, the system correctly categorised 85 images as Block, but the system incorrectly classified 0 images which is an error.

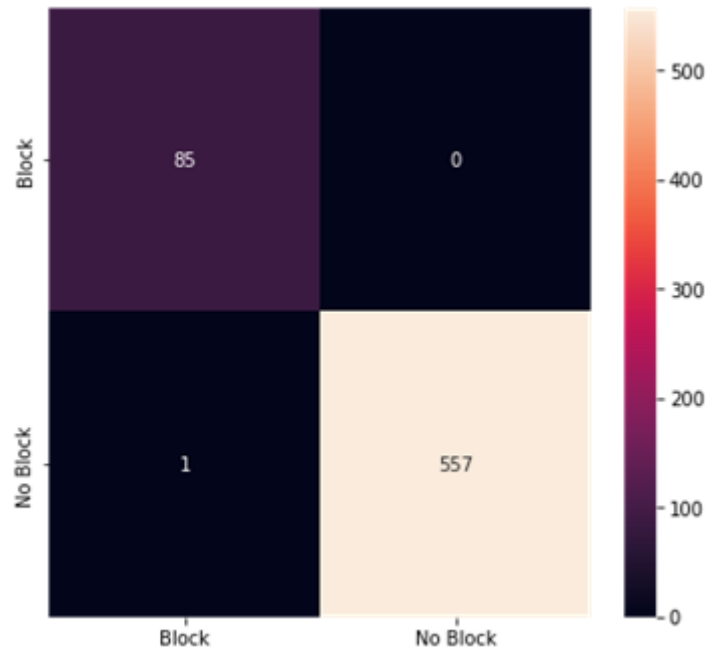


Figure 5.30: Confusion Matrix of Ensemble Model Architecture

5.4.2 Multiclass Classification

ResNet50

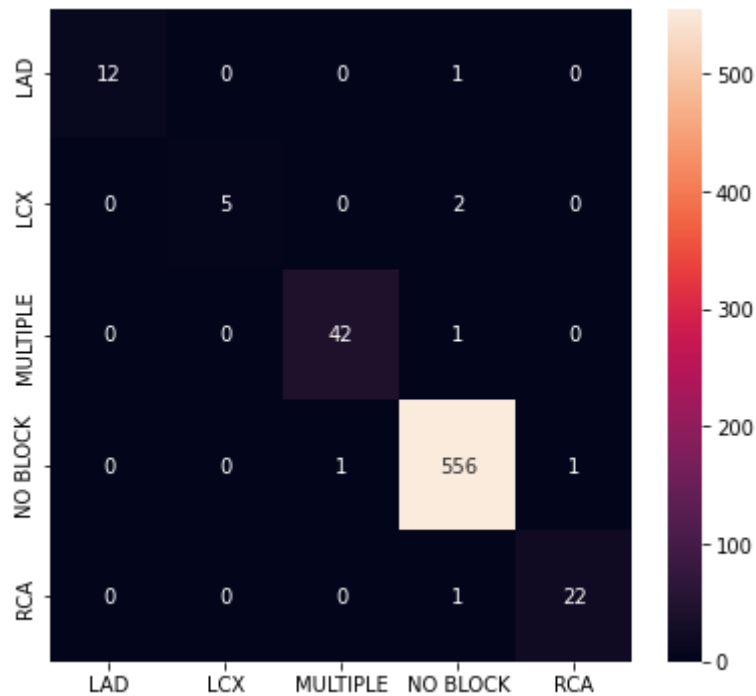


Figure 5.31: Confusion Matrix of ResNet50

In the above figure the confusion matrix of Resnet50 is picturized. The algorithm could correctly classify 12 LAD, 5 LCX, 22 RCA, 42 Multiple and 556 No block images. And incorrectly classified 1 LAD, 2 LCX, 1 MULTIPLE and 1 RCA as No

block . Then for 1 No block each for Multiple and RCA.

VGG16

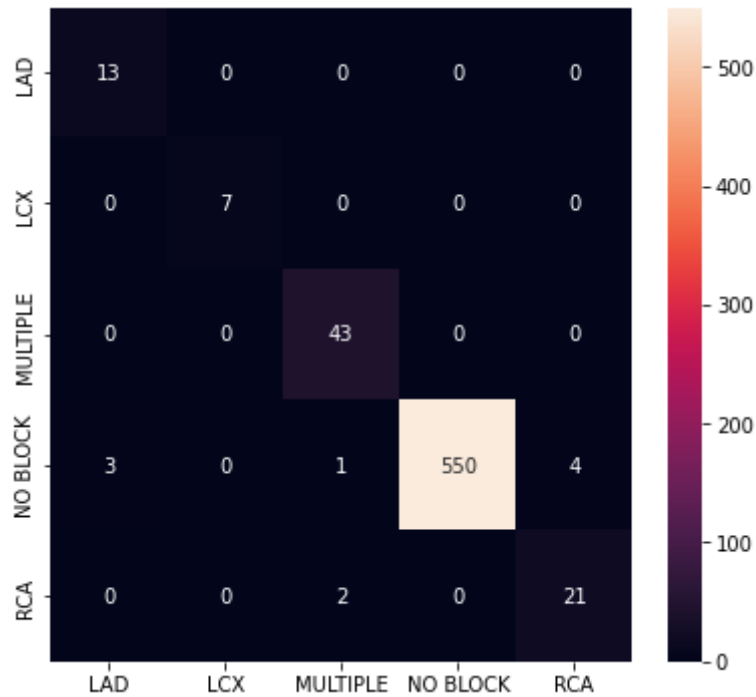


Figure 5.32: Confusion Matrix of VGG16

In the above figure the confusion matrix of VGG16 is illustrated. The algorithm could correctly classify 13 LAD, 7 LCX, 21 RCA, 43 Multiple and 550 No block images. And incorrectly classified 3 No block as LAD, 1 No block as Multiple 4 No block as RCA. Lastly 2 RCA as Multiple.

VGG19

In the figure the confusion matrix of VGG19 is illustrated. The algorithm could correctly classify 10 LAD, 7 LCX, 21 RCA, 43 Multiple and 556 No block images. And incorrectly classified 1 No block each for LAD and Multiple. Lastly 2 RCA as No block.

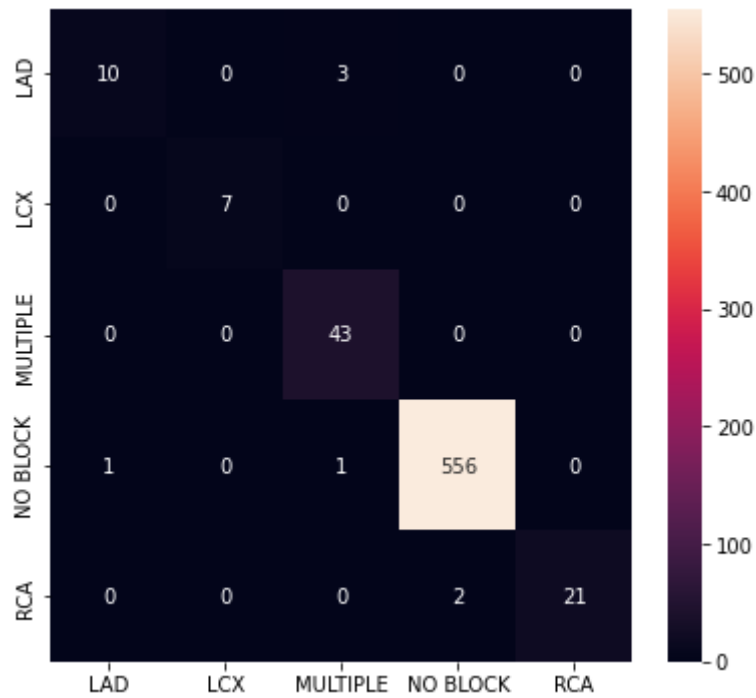


Figure 5.33: Confusion Matrix of VGG19

Inception V3

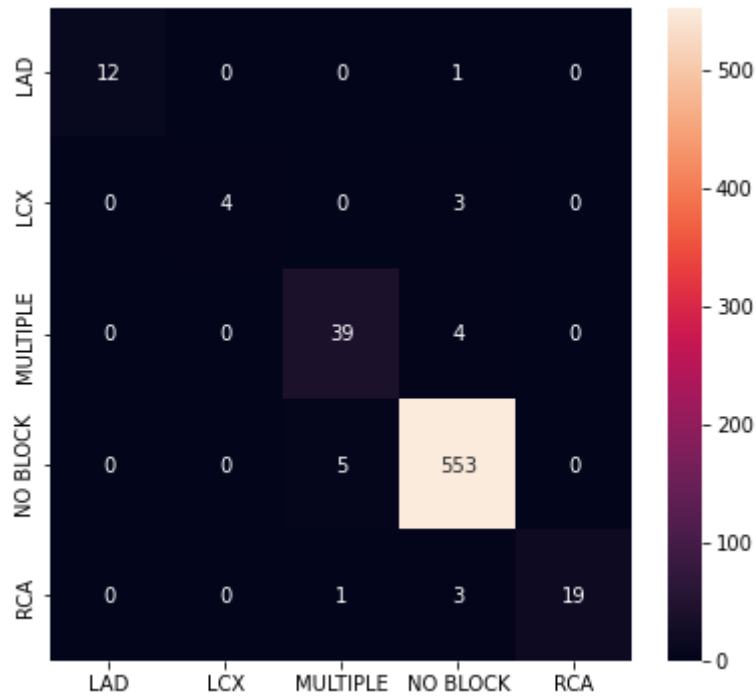


Figure 5.34: Confusion Matrix of Inception V3

In the confusion matrix of Inception V3 , the algorithm classified 12 LAD, 4 LCX, 19 RCA, 29 Multiple and 553 No block images. But was incorrect in classifying 1 LAD, 3 LCX, 4 Multiple and 3 RCA as No block. Along with 5 No blocks and 1

RCA as Multiple.

DenseNet121

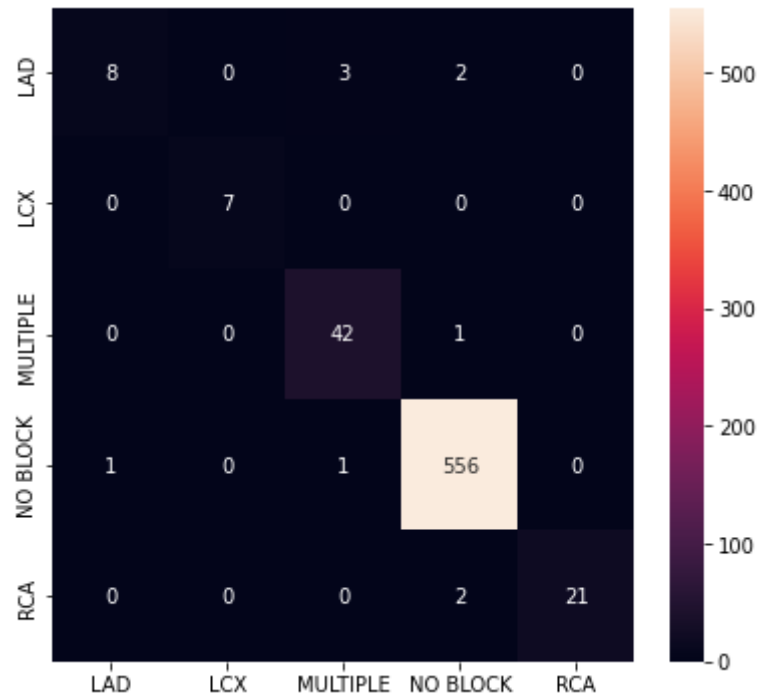


Figure 5.35: Confusion Matrix of DenseNet121

In the confusion matrix of DenseNet121 , the algorithm classified 8 LAD, 7 LCX, 21 RCA, 42 Multiple and 556 No block images. But was incorrect in classifying 3 LAD, 1 No block. Along with 5 No blocks as Multiple and 2 LAD, 1 Multiple and 2 RCA as No block.

Ensemble Model

In the illustration of the confusion matrix of the Ensemble model, the algorithm could classify 10 LAD, 7 LCX, 21 RCA, 42 Multiple and 557 No block images accurately. On the other hand, 2 LAD and 1 No block as Multiple. Along with 1 LAD, 1 Multiple and 2 RCA as No block.

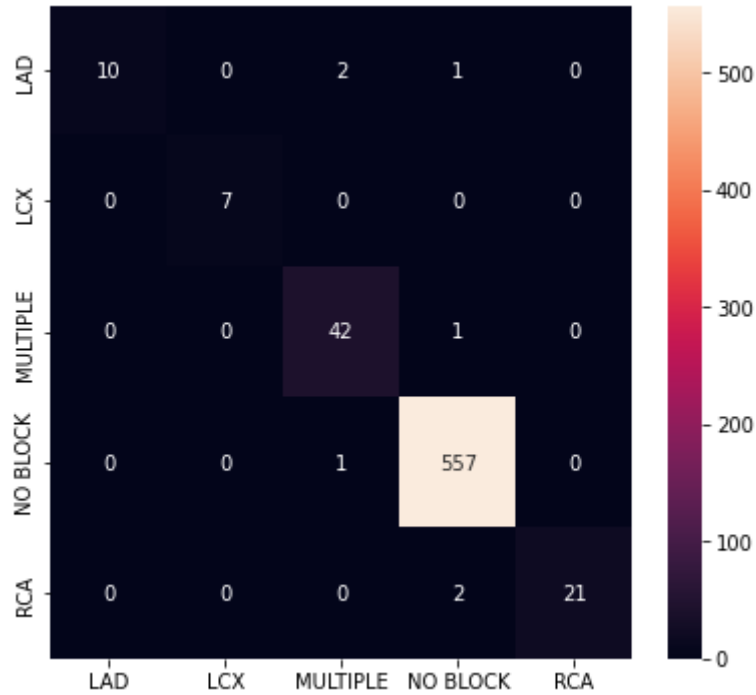


Figure 5.36: Confusion Matrix of Ensemble Model Architecture

5.5 Result Analysis

In our study, we have analysed angiogram datasets and did Binary and multiclass classification. In both the models, we have implemented ResNet50, VGG16, VGG19, Inception V3 and DenseNet121.

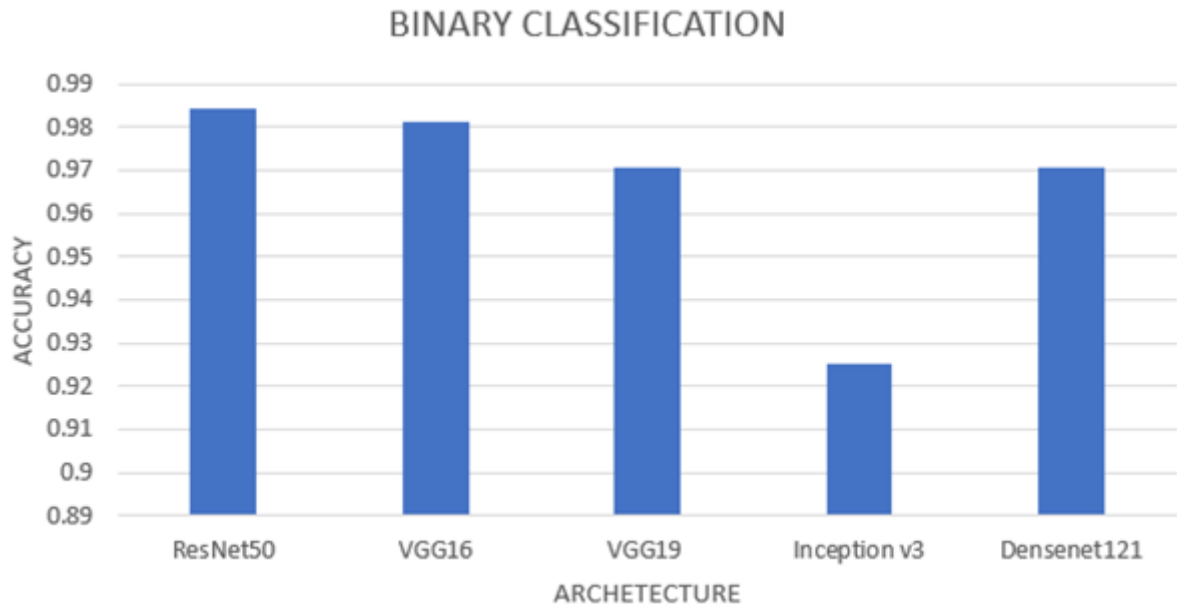


Figure 5.37: Accuracy of Binary classification of different architectures

In case of Binary classification, there were 2 classes and here we got accuracy of 98.44% for ResNet50, 98.13% for VGG16, 97.05% for VGG19, 92.53% for Inception

BINARY CLASSIFICATION

Architecture	Accuracy	Precision	Recall	F1 Score
ResNet50	98.44%	98.43%	98.44%	98.42%
VGG16	98.13%	98.11%	98.13%	98.11%
VGG19	97.05%	97.43%	97.05%	97.14%
InceptionV3	92.53%	92.91%	92.53%	91.30%
DenseNet121	97.05%	97.10%	97.05%	97.07%

Figure 5.38: Comparison of Binary classification of different architectures

V3 and 97% for DenseNet121. So, here ResNet50 out performed the other architectures. And by taking train and validation in consideration the top three are ResNet50, VGG16 and VGG19.

MULTICLASS CLASSIFICATION

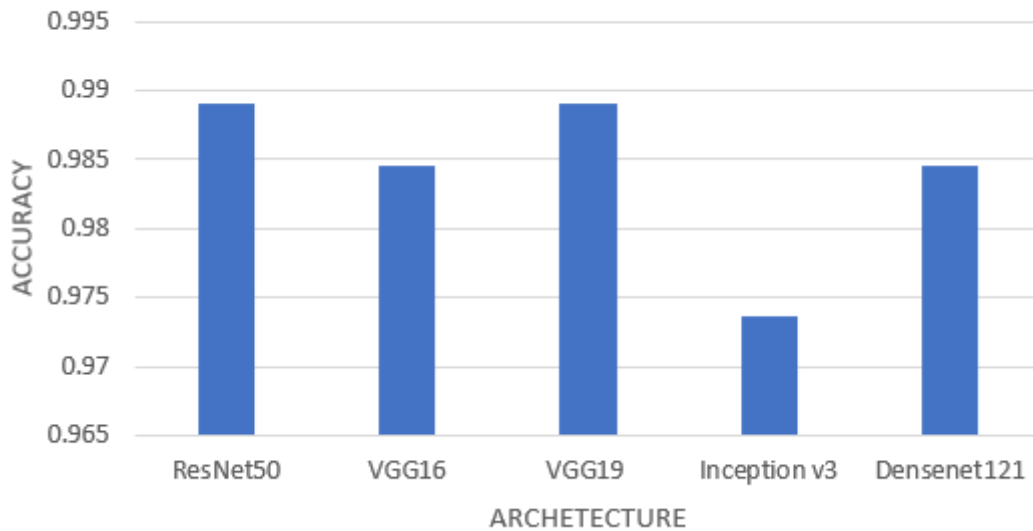


Figure 5.39: Accuracy of Multiclass classification of different architectures

Similarly, for Multiclass classification we have splitted the dataset into 5 classes. And achieved an accuracy of 98.91% for ResNet50, 98.45% for VGG16, 98.91% for VGG19, 97.36% for Inception V3 and 98.45% for DenseNet121. By taking train and validation in consideration among the 5 models VGG19 has the best accuracy. And the top three models are ResNet50, VGG19 and DenseNet121.

MULTICLASS CLASSIFICATION

Architecture	Accuracy	Precision	Recall	F1 Score
ResNet50	98.91%	98.91%	98.91%	98.88%
VGG16	98.44%	98.61%	98.44%	98.49%
VGG19	98.91%	98.93%	98.91%	98.89%
InceptionV3	97.36%	97.42%	97.36%	97.28%
DenseNet121	98.44%	98.42%	98.44%	98.37%

Figure 5.40: Comparison of Multiclass classification of different architectures

Finally, taking the top three architectures we have implemented the Ensemble model architecture for Binary classification and Multiclass classification where we got an accuracy of 99.84% and 98.91% respectively.

Ensemble Model							
BINARY CLASSIFICATION				MULTICLASS CLASSIFICATION			
Accuracy	Precision	Recall	F1 Score	Accuracy	Precision	Recall	F1 Score
99.84	99.85	99.84	99.84	98.91	98.93	98.91	98.88

Figure 5.41: Accuracy of Ensemble Model Architecture

5.6 Result Comparison

Comparing our study with the paper by Zhanchao Xian Et al. on their study of “Main Coronary Vessel Segmentation using Deep Learning in Smart Medical” we identify massive differences in the results and study methodology. Comparing these studies, it clearly represents diverse results in studies, not only on results but the approach to reach the conclusion is also different. The architecture and models used to implement the study are different as they have used UNet, Residual Attention Network which are different from our approach to this study. In contrast to the results gained by Zhanchao Et al. we achieved better precision (Pre), recall (Re) and F1 Score. Evaluating 3200 Images they achieved a score of 0.901, 0.898 and 0.90 respectively for the precision, recall and F1 score. Whereas, we gained a better accuracy 0.9984 as well as precision 0.9985, recall 0.9984 and F1 Score of 0.9984

for evaluating our results for binary class. For our Multiclass classification we also achieved better results than them.[31]

Similarly, Comparing our study with the research done by Su Yang Et al. on their topic “Deep Learning segmentation of major vessels in X-ray coronary angiography” it is seen that the results are different as well as they have used UNet model along with other models like ResNet101 to evaluate their results, which are different models than the models we have used. Moreover, they have used only F1 score as evaluation matrix whereas, we evaluated our models based on accuracy. precision, recall and F1 Score. We achieved an F1 score of 0.9984 and 0.9888 for binary classification and multiclass classification which is more than 0.9. To mention their achieved value, they achieved 0.917 F1 Score. We used many different models ResNet50, VGG16, VGG19, Inception V3, DenseNet121 and achieved different values. Finally, using the Ensemble learning model we achieved our desired results.[32]

Chapter 6

Conclusion and Future Prospect

Coronary artery disease is also known as ischemic heart disease is enlisted as the most prominent heart disease in the world claimed by World Health Organization (WHO). Coronary artery disease has caused the most deaths worldwide and is responsible for 16% of the total deaths worldwide. The diagnosis protocol for this coronary artery disease is a lengthy and invasive process. Due to such a long time taken for the diagnosis of coronary artery blockage, patients many times do not receive appropriate treatment at an early stage. As a result, to ensure the diagnosis of coronary heart disease at an early stage, our model enables identification and diagnosis of coronary artery blockage at an early stage by evaluating the Angiogram images of the heart. Throughout our study, we were able to collect a dataset of angiograms (Angiogram images) of the Heart. We pre-processed the dataset for implementation to our model for the diagnosis of coronary artery blockage. Based on the severity of the blockage, cardiologists can determine if the patient requires an angioplasty, bypass surgery, or no surgery at all. Furthermore, in our research model, we utilized an Ensemble Learning Model along with multi-class classification which will detect artery blockage with increased accuracy. Thus, our model will lead to the detection of coronary artery blockage with higher accuracy and minimal error at an early stage. This will result in patients gaining accurate treatment and help save the lives of patients endangered with heart risks.

Moreover, it is intended to work on this proposed model by collecting more resources for the betterment of the medical science to a greater extent. To conclude, this research is yet to be further developed for the sake of revolution in medical science. This research can be evaluated furthermore by using different large-scale datasets and enhanced algorithms to bring innovation to the medical science sector.

Bibliography

- [1] N. H. S. (NHS), UK. (2019, 11/13/19). "Coronary artery disease"
- [2] WHO, "Cardiovascular diseases," World Health Organization (2019)
- [3] S. W. Reinhardt, C.-J. Lin, E. Novak, and D. L. Brown, "Noninvasive Cardiac Testing vs Clinical Evaluation Alone in Acute Chest Pain: A Secondary Analysis of the ROMICAT-II Randomized Clinical Trial," (in eng), *JAMA internal medicine*, vol. 178, no. 2, pp. 212-219, 2018.
- [4] S. Kohsaka and A. N. Makaryus, "Coronary Angiography Using Noninvasive Imaging Techniques of Cardiac CT and MRI," (in eng), *Current cardiology reviews*, vol. 4, no. 4, pp. 323-330, 2008.
- [5] CDC, USA(January 11, 2021) "Heart Attack Symptoms, Risk, and Recovery"
- [6] Johns Hopkins Medicine, "Heart Attack"
- [7] Salma S., M. A. Azim, A. A. Raouf, "Narrowed coronary artery detection and classification using angiographic scans", 2017 12th International Conference on Computer Engineering and Systems (ICCES)
- [8] S. B. Mudigoudar and A. I. Rasheed, "Design and implementation of image processing algorithms for cardiac blockage detection on FPGA," 2016 IEEE Annual India Conference (INDICON), pp. 1-5, 2016.
- [9] Roohallah A. , Mohammad H. Z.,M. J. Hosseini,Jafar H., Abbas K., M. Roshanzamir , Fahime K., Nizal S. , Saeid N. , "Coronary Artery Disease Detection Using Computational Intelligence Methods", *Knowledge-Based Systems*, Vol. 109 pp.187-197, 2016.
- [10] C.Gaudio, F.Mirabelli, F.Pelliccia, M.Francone, G.Tanzili, S.D. Michele, S.Leonetti, G.D.Vincentis, I.Carbone, E.Mangieri, C.Catalano, R. Passariello, "Early detection of coronary artery disease by 64-slice multidetector computed tomography in asymptomatic hypertensive high-risk patients", *International Journal of Cardiology*, vol. 135, pp. 280-286, 2009.
- [11] F. Ahmed, F.T.Johora, R.J. Chakma, S. Hossain, D. Sarma, "A Combined Belief Rule based Expert System to Predict Coronary Artery Disease", *International Conference on Inventive Computation Technologies (ICICT-2020)*
- [12] U. Rajendra Acharya, Hamido Fujita, Oh Shu Lih, Muhammad Adam, Jen Hong Tan, Chua Kuang Chua, "Automated detection of coronary artery disease using different durations of ECG segments with convolutional neural network", *Knowledge-Based-Systems*, Volume 132, 15 September 2017, Pages 62-71.

- [13] Abdallah Y., Tariq A. “Improvement of sonographic appearance using HAT-TOP methods.” *International Journal of Science and Research (IJSR)*. 2015; 4(2): 2425-2430
- [14] Batenburg KJ, Sijbers J. Adaptive thresholding of tomograms by projection distance minimization. *Pattern Recognition*. 2009;42(10): 2297-2305. DOI: 10.1016/j.patcog.2008.11.027
- [15] S. I. Ayon, Md. M. Islam Md. Rahat H. (2020): “Coronary Artery Heart Disease Prediction: A Comparative Study of Computational Intelligence Techniques”, *IETE Journal of Research*, DOI: 10.1080/03772063.2020.1713916
- [16] N Swanson, G Montalescot, K A Eagle, S G Goodman, W Huang, D Brieger, G Devlin (2013), “Delay to angiography and outcomes following presentation with high-risk, non-ST-elevation acute coronary syndromes: results from the Global Registry of Acute Coronary Events”
- [17] Manesh R.Patel, Eric D. Peterson, M.D., M.P.H., David Dai, M.S., Matthew Brennan, M.D., Rita F. Redberg, M.D., H. Vernon Anderson, M.D., Ralph G. Brindis, M.D., Pamela S. Douglas, M.D. “Low Diagnostic Yield of Elective Coronary Angiography” 10.1056/NEJMoa0907272
- [18] Suleyman E., Mehmet K., Kazim A., Vedat D. “Sudden death after normal coronary angiography and possible causes” Gaziantep University, Turkey. doi: 10.1136/bcr-2013-008753
- [19] Peter E. and Barbara H., “Doctors perform thousands of unnecessary surgeries” *USA Today*.
- [20] Kurama, V. (2021, April 9). A Guide to AlexNet, VGG16, and GoogleNet. *Paperspace Blog*. <https://blog.paperspace.com/popular-deep-learning-architectures-alexnet-vgg-googlenet/>
- [21] ResNet, AlexNet, VGGNet, Inception: Understanding various architectures of Convolutional Networks. (2017, August 9). *CV-Tricks.Com*.
- [22] EfficientNet: Improving Accuracy and Efficiency through AutoML and Model Scaling. (2019, May 29). *Google AI Blog*.
- [23] Lessons learned from reproducing ResNet and DenseNet on CIFAR-10 dataset. *Medium*. (2018a, October 11).
- [24] P. Mirunalini, C. Aravindan, A. Thamizh Nambi, Poorvaja. S and Pooja Priya. V, “Segmentation of Coronary Arteries from CTA axial slices using Deep Learning techniques” (2019) Dept. of Computer Science, SSN College of Engineering, Chennai, India DOI:10.1109/TENCON.2019.8929260
- [25] Semmlow, J., Rahalkar, K. (2007). Acoustic Detection of Coronary Artery Disease. *Annual Review of Biomedical Engineering*, 9(1), 449–469.
- [26] T.Du, X.Liu, H.Zhang, B.Xu, “ Real-time Lesion Detection of Cardiac Coronary Artery Using Deep Neural Networks” *Pattern Recognition and Intelligent System Lab Beijing University of Posts and Telecommunications*, Beijing 100876, China

- [27] Sun, Z., Jiang, W. (2006). Diagnostic value of multislice computed tomography angiography in coronary artery disease: A meta-analysis. *European Journal of Radiology*, 60(2), 279–286.
- [28] A. Rosebrock, "ImageNet: VGGNet, ResNet, Inception, and Xception with Keras", 2017 Link: <https://pyimagesearch.com/2017/03/20/imagenetvggnet-resnet-inception-xception-keras/>
- [29] Z. Jaadi, step-by-step explanation of principal component analysis (pca)," Retrieved June, vol. 7, p. 2021, 2021.
- [30] S. Wold, K. Esbensen, and P. Geladi, component analysis," *Chemometrics and intelligent laboratory systems*, vol. 2, no. 1-3, pp. 37(52), 1987.
- [31] Main Coronary Vessel Segmentation Using Deep Learning in Smart Medical. (2020, October 22). Retrieved September 18, 2022, <https://www.hindawi.com/journals/mpe/2020/8858344/>
- [32] Yang, S. (2019, November 15). Deep learning segmentation of major vessels in X-ray coronary angiography. *Nature*. Retrieved September 18, 2022, from
- [33] S. M. Anwar, M. Majid, A. Qayyum, M. Awais, M. Alnowami, and M. K. Khan, "Medical image analysis using convolutional neural networks: A review," *Journal of medical systems*, vol. 42, no. 11, pp. 1–13, 201
- [34] S. Sharma, S. Sharma, and A. Athaiya, "Activation functions in neural networks," *towards data science*, vol. 6, no. 12, pp. 310–316, 20
- [35] R. Arora, A. Basu, P. Mianjy, and A. Mukherjee, "Understanding deep neural networks with rectified linear units," *arXiv preprint arXiv:1611.01491*, 2016.
- [36] M. Wang, S. Lu, D. Zhu, J. Lin, and Z. Wang, "A high-speed and low complexity architecture for softmax function in deep learning," in *2018 IEEE Asia Pacific Conference on Circuits and Systems (APCCAS)*, IEEE, 2018, pp. 223–226.